A review of the relationships describing the signal of a Large Aperture Scintillometer

A.F. Moene, W.M.L. Meijninger, O.K. Hartogensis, W. Kohsiek, H.A.R. de Bruin

March 2004

Internal report 2004/2

Meteorology and Air Quality Group
Wageningen University
Duivendaal 2
6701 AP Wageningen
The Netherlands
http://www.met.wau.nl

This work has been sponsored by the Dutch Technology Foundation STW (WMO4133)

WAGENINGEN UNIVERSITEIT
WAGENINGEN UR

Contents

1 Introduction

The Large Aperture Scintillometer (LAS) has been developed in the 1970's (Wang *et al.*, 1978). It has been applied to measure a number of atmospheric surface layer quantities, most notably the structure function parameter of the refractive index, C_{n^2} (Ochs and Wang, 1978), the wind speed across the scintillometer path (Ochs *et al.*, 1976) and the inner scale of turbulence (Hill and Ochs, 1978; Hartogensis *et al.*, 2002). The present paper will deal with the derivation of the sensible heat flux from LAS data (Wesely, 1976*b*; de Bruin *et al.*, 1995; Meijninger *et al.*, 2002*b*; Kohsiek *et al.*, 2002).

The LAS consists of a transmitter and a receiver which are separated by a distance L, the path length. The transmitter and and receiver have finite aperture diameters (D_t and D_t) which are 'large' (the meaning of the word large will become clear in the course of this paper). The radiation emitted by the transmitter is scattered by the turbulent medium between the transmitter and the receiver. The receiver collects both the undisturbed beam of the transmitter and the scattered radiation (see figure 1.1). It is the fluctuation of the scattered light that carries information about the turbulent field along the scintillometer path.

The aim of this paper is to show and clarify the theory and assumptions that underly the derivation of sensible heat flux from LAS measurements. The link between LAS data and the sensible heat flux consists of three steps, which will be the subject of subsequent sections:

- From the signal of the LAS the structure function parameter of the refractive index can be inferred, which is shown in section 2.4). Since that section heavily relies on turbulence theory, it is preceded by a section that deals with the statistical description of a turbulent field. Both vector and scalar fields are dealt with (section 2).
- The structure parameter of the refractive index –obtained in the first step– can be related to the structure function parameter of temperature. Section 3 deals with the properties of air that cause variations in the refractive index and shows the relationship between the structure function parameters of the refractive index and temperature.
- Finally, the structure function parameter of temperature can be related to the sensible heat flux through similarity relationships. This step is discussed in 4.

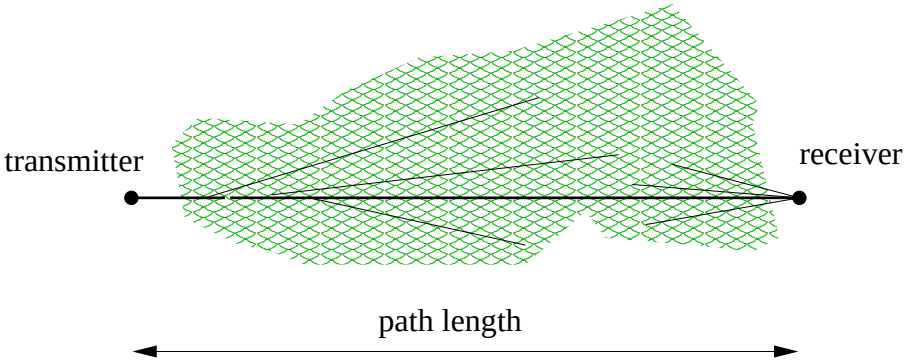

Figure 1.1: The LAS consists of a transmitter and a receiver, a given distance apart (path length). The radiation produced by the transmitter is scattered by the turbulent medium between transmitter and receiver. The receiver collects both the undisturbed beam of the transmitter and the scattered radiation.

All discussions are centred around the LAS as it is built and used by the Meteorology and Air Quality Group of Wageningen University. Thus this paper is not intended to be a full review of all aspects of scintillometry.

2 Statistical description of a turbulent field

2.1 Statistical tools

Since turbulent flows are not reproducible in detail, they can be described in a statistical sense only. In this section the statistical properties used in this report will be discussed[1]. Some of the statistical properties are defined in terms of the deviation of a random variable (say u), u'. This deviation is defined by the Reynolds decomposition:

$$u = \overline{u} + u' \,, \tag{2.1}$$

where $\overline{u}$ is a mean value and u' is the deviation from that mean. In the sequel it will be assumed that $\overline{u}$ is the *ensemble average* (see Monin and Yaglom (1971) for the general requirements for this average).

The random variable $u(\boldsymbol{r})$ can be described with the statistical moments $B_{uu\ldots u}$ where $\boldsymbol{r}$ is a point in four-dimensional space (space and time). In general, the k-th order moments are the mean values of products of k values of the field (Monin and Yaglom, 1971):

$$B_{uu\ldots u}(\boldsymbol{r}_1, \boldsymbol{r}_2, \ldots, \boldsymbol{r}_k) = \overline{u'(\boldsymbol{r}_1)u'(\boldsymbol{r}_2)\ldots u'(\boldsymbol{r}_k)} \tag{2.2}$$

In most applications it is assumed that the random variables under consideration are strongly stationary [2] in all directions $\boldsymbol{r}_l - \boldsymbol{r}_m$ where l and m can be any combination with $l, m < k$. This implies that statistical quantities are independent of position on lines or planes through $\boldsymbol{r}_1 \ldots \boldsymbol{r}_k$. When this requirement is too strict one can revert to the assumption of stationary increments: the difference $u(\boldsymbol{r}_1) - u(\boldsymbol{r}_2)$ is assumed to be —at least weakly— stationary (see Strohbehn (1968) for an example of the advantage of the structure function over the correlation function). This implies that the difference $u(\boldsymbol{r}_1) - u(\boldsymbol{r}_2)$ is determined mainly by inhomogeneities with a scale less than $|\boldsymbol{r}_1 - \boldsymbol{r}_2|$

The structure of such random field with stationary increments can be described with the structure function (Tatarskii, 1961):

$$D_{uu\ldots u}(\boldsymbol{r}_1, \boldsymbol{r}_2) = \overline{(u(\boldsymbol{r}_1) - u(\boldsymbol{r}_2))\,(u(\boldsymbol{r}_1) - u(\boldsymbol{r}_2))\ldots(u(\boldsymbol{r}_1) - u(\boldsymbol{r}_2))} \,. \tag{2.3}$$

The order of the structure function is determined by the number of increments used in the multiplication. In the present application only the second order structure function will be used:

$$D_{uu}(\boldsymbol{r}_1, \boldsymbol{r}_2) = \overline{(u(\boldsymbol{r}_1) - u(\boldsymbol{r}_2))\,(u(\boldsymbol{r}_1) - u(\boldsymbol{r}_2))} \,.$$

Since the increments are stationary, the dependence on $\boldsymbol{r}_1$ and $\boldsymbol{r}_2$ can be replaced by a dependence on the distance $\boldsymbol{r} = |\boldsymbol{r}_1 - \boldsymbol{r}_2|$ only

$$D_{uu}(\boldsymbol{r}_1, \boldsymbol{r}_2) = D_{uu}(\boldsymbol{r}) \,.$$

[1] Only statistical properties of one variable will be discussed

[2] A random variable is weakly stationary in a given direction if the ensemble mean and the auto-covariance function are independent of position in that direction. Strong stationarity implies that all statistical quantities are independent of position in the stationary direction (see Bendat and Piersol (1986))

In the case of a random field with stationary increments, homogeneity and isotropy can be assumed to apply *locally* only. See Kolmogorov (1941*b*) for a definition of local homogeneity and isotropy.

To conclude this section, the link between the structure function and two other statistical quantities will be given (under the assumption of isotropy for the sake of simplicity). The link between the second order structure function D_{uu} and the second order moment B_{uu} can only be shown for a strictly homogeneous random field (since B_{uu} only makes sense under homogeneous conditions). Then:

$$D_{uu}(r) = 2\left(B_{uu}(0) - B_{uu}(r)\right) \tag{2.4}$$

The structure function can also be expressed in terms of the three-dimensional spectral density[3] $\Phi_{uu}(\kappa)$ as (Tatarskii, 1961):

$$D_{uu}(r) = 8\pi \int_0^\infty \left(1 - \frac{\sin \kappa r}{\kappa r}\right) \Phi_{uu}(\kappa)\kappa^2 d\kappa \,, \tag{2.5}$$

where κ is the magnitude of the wave number. For this expression only *local* homogeneity (and isotropy) has to be assumed.

2.2 Structure function of a turbulent velocity field

2.2.1 Structure function of an arbitrary velocity field

The structure function of a vector field $\boldsymbol{u}$ is a second order tensor with components $D_{u_i u_j}$ in a Cartesian coordinate system:

$$D_{u_i u_j}(\boldsymbol{r}) = \overline{(u_i(\boldsymbol{r}_1) - u_i(\boldsymbol{r}_2))(u_j(\boldsymbol{r}_1) - u_j(\boldsymbol{r}_2))} \,, \tag{2.6}$$

where u_i is the velocity component in the i-direction. The separation vector $\boldsymbol{r}$ has components r_i. Two components of $D_{u_i u_j}$ have special significance:

- Longitudinal structure function $D^{\parallel}_{u_i u_i}$ if $\boldsymbol{r} \parallel u_i$;
- Transverse structure function $D^{\perp}_{u_i u_i}$ if $\boldsymbol{r} \perp u_i$;

In the case of local isotropy, it can be derived Kolmogorov (1941*b*) that $D_{u_i u_j}$ has the following form:

$$D_{u_i u_j}(\boldsymbol{s}) = \left(D^{\parallel}_{uu}(s) - D^{\perp}_{uu}(s)\right) n_i n_j + D^{\perp}_{uu}(s)\delta_{ij} \,, \tag{2.7}$$

where n_i are the components of the unit vector $\boldsymbol{n}$ parallel to $\boldsymbol{r}$ and δ_{ij} is the Kronecker delta (equalling 1 for $i = j$ and zero otherwise). When —additionally— the flow can be assumed to be incompressible, an extra condition on $D_{u_i u_j}(\boldsymbol{r})$ can be imposed:

$$\frac{\partial D_{u_i u_j}}{\partial r_i} = 0 \,. \tag{2.8}$$

Combination of (2.7) and (2.8) leads to:

$$D^{\perp}_{uu} = \frac{1}{2r}\frac{d}{dr}(r^2 D^{\parallel}_{uu}) \,, \tag{2.9}$$

so that $D_{u_i u_j}$ can be expressed in either $D^{\parallel}_{uu}$ or $D^{\perp}_{uu}$.

[3] Here a three-dimensional spectral density, denoted by Φ_{xx} is the three-dimensional Fourier transform of a three-dimensional covariance function. A one-dimensional spectral density (F_{xx}) is the one-dimensional Fourier transform of a one-dimensional covariance function (which may be one-dimensional due to isotropy). Φ_{xx} and F_{xx} are related by $\Phi_{xx} = -\frac{1}{2\pi\kappa}\frac{\partial F_{xx}}{\partial \kappa}$. For more details see Strohbehn (1968)

2.2.2 Structure function of a turbulent velocity field

The structure function of a *turbulent* velocity field has a number of features that will be described in this section. In this analysis two length scales play a role:

- The inner-scale l_0, which is the length scale of the smallest eddies (those for which the Reynolds number $Re_{l_0} = v_0 l_0/\nu$ equals 1). l_0 can be related to the dissipation rate as:

$$l_0 = (\nu^3/\epsilon)^{1/4} \,. \tag{2.10}$$

- The outer scale $\mathcal{L}_0$ which is related to the size of the flow domain.

According to the two similarity hypotheses of Kolmogorov (1941*b*) the following statements can be made about the structure functions:

- 1If the separation $r = |\boldsymbol{r}|$ is small compared to the outer scale ($r \ll \mathcal{L}_0$), then the structure function is determined by the kinematic viscosity ν and the average energy dissipation ϵ.
- 2If, additionally the separation r is large compared to the inner-scale l_0(i.e. r is within the inertial subrange) then the structure function is uniquely determined by the energy dissipation ϵ .

For the case where $r \ll l_0$ it can be assumed that the velocity increments are a smooth function of r (expansion of $u_i(r_1) - u_i(r_2)$ in a power series, retaining only the first term: $u_i(r_1) - u_i(r_2) \sim \alpha r$, with α a constant) and thus $D^{\perp}_{uu} \sim r^2$ (Kolmogorov, 1941*a*). Dimensional arguments then lead to the following forms for the structure function (where the values of constant of proportionality is specific to the longitudinal structure function):

$$D^{\parallel}_{uu}(r) = \frac{1}{15}\frac{\epsilon}{\nu} r^2 \qquad l_0 \ll r \,, \tag{2.11a}$$

$$D^{\parallel}_{uu}(r) = C\epsilon^{2/3} r^{2/3} \qquad l_0 \gg r \gg \mathcal{L}_0 \,, \tag{2.11b}$$

The transverse structure function can be derived from (2.11) using the incompressibily relationship (2.9).

One could use the expressions (2.11a) and (2.11b) to define the inner scale l_0 as the value of r where the two expressions for $D^{\parallel}_{uu}(r)$ intersect. This leads to :

$$l_0 = \sqrt[4]{(15C\nu)^3/\epsilon} \,. \tag{2.12}$$

With this definition of l_0 (which equals (2.10) provided $C = 1/15$) (2.11) can be rewritten as:

$$D^{\parallel}_{uu}(r) = C_{u^2}\epsilon^{2/3} l_0^{1/4} \left(\frac{r}{l_0}\right)^2 \qquad l_0 \ll r \,, \tag{2.13a}$$

$$D^{\parallel}_{uu}(r) = C_{u^2} r^{2/3} \qquad l_0 \gg r \gg \mathcal{L}_0 \,, \tag{2.13b}$$

where $C_{u^2} = \frac{1}{15\nu} l_0^{3/4} \epsilon^{1/3}$ [4] .

2.3 Structure function for a scalar

In order to derive the structure functions for a scalar quantity (say θ), the inhomogeneities in that scalar have to be quantified. Tatarskii (1961) does this on the basis of dimensional arguments in the following way.

The largest inhomogeneities in the distribution of θ are caused by the largest scales of the turbulent field with length scale larger than $\mathcal{L}_0$. At these large scales the scalar fluctuation is produced at a rate $\overline{N}$. These large scale fluctuations break up in fluctuations with a smaller spatial scale, until the size of the fluctuations is such that they are dissipated (at a rate $\overline{N}$). Since the turbulent velocity field is anisotropic

[4] With respect to the notation of the structure function parameter (and especially cross-structure function parameter) some confusion exists. In the present paper, the index of C shows to which variables the structure function parameter refers: e.g. C_{TT} or C_{T^2} is the temperature structure function parameter and C_{Tq} is the temperature-humidity cross-structure function parameter. . A more commonly used notation is C_T^2, C_{Tq} and C_q^2.

at scales $\mathcal{L} \gg \mathcal{L}_0$, the scalar fluctuations will be anisotropic as well. However, the fluctuations at smaller scales can be considered isotropic. The difference $\theta(\boldsymbol{r}_1) - \theta(\boldsymbol{r}_2)$ is mainly determined by fluctuations at scales which are less than $|\boldsymbol{r}_1 - \boldsymbol{r}_2|$, so that for $|\boldsymbol{r}_1 - \boldsymbol{r}_2| \ll \mathcal{L}_0$ the field $\theta(\boldsymbol{r})$ is a locally isotropic random field.

Parallel to the two hypotheses of Kolmogorov (1941*b*) with respect to a locally isotropic velocity field two hypotheses can be stated for the scalar fluctuations (see Obukhov (1949); Corrsin (1951)).

- 1If the separation $r = |\boldsymbol{r}|$ is small compared to the outer scale ($r \ll \mathcal{L}_0$), then the structure function D_θ is determined by the molecular diffusion coefficient D and the average scalar fluctuation dissipation $\overline{N}$.
- 2If, additionally the separation r is large compared to the inner-scale l_0(i.e. r is within the inertial subrange) then the structure function is uniquely determined by the scalar fluctuation dissipation $\overline{N}$

At scales less than the inner scale l_0 the difference $(\theta(\boldsymbol{r}_1) - \theta(\boldsymbol{r}_2))$ will be a smooth function of r so that $D_{\theta^2} \sim r^2$ (see section 2.2.2).

On the basis of dimensional arguments and more detailed considerations the following forms for the structure function can be derived:

$$D_{\theta^2}(r) = \frac{1}{3}\frac{\overline{N}}{D} r^2 \qquad r \ll l_0 \,, \tag{2.14a}$$

$$D_{\theta^2}(r) = a^2 \frac{\overline{N}}{\epsilon^{1/3}} r^{2/3} \qquad l_0 \ll r \ll \mathcal{L}_0 \,. \tag{2.14b}$$

The inner scale l_0 can be defined as value of r where (2.14a) and (2.14b) intersect. This leads to $l_0 = \sqrt[4]{27 a^6 D^3/\epsilon}$ (note that this l_0 is not necessarily equal to that derived for the velocity field (2.10) or (2.12)). Equation (2.14) can now be rewritten as:

$$D_{\theta^2}(r) = C_{\theta^2} l_0^{2/3} \left(\frac{r}{l_0}\right)^2 \qquad r \ll l_0 \,, \tag{2.15a}$$

$$D_{\theta^2}(r) = C_{\theta^2} r^{2/3} \qquad l_0 \ll r \ll \mathcal{L}_0 \,, \tag{2.15b}$$

where $C_{\theta^2} = a^2 \overline{N} \epsilon^{-1/3}$. C_{θ^2} is called the structure function parameter or structure function parameter for scalar θ.

2.4 C_{n^2} derived from Large Aperture Scintillometer data

The Large Aperture Scintillometer (LAS) can be used to measure the structure parameter of the refractive index n, C_{n^2}, which can in turn be linked to the structure function parameter for temperature, C_{T^2}. In the forthcoming sections the link between the signal of the LAS and C_{n^2} will be shown, whereas the link between C_{n^2} and C_{T^2} will be the subject of section 3.

In this section a mathematical description of the signal at the detector of the LAS is contructed. The first step is the description of the log-amplitude variance resulting when a spherical wave pased through a random medium. Both the cases of weak and strong scattering are considered (subsections 2.5) and 2.5.1). In section 2.6 the relationship between the signal of the LAS (log-intensity variance) and C_{n^2} is derived, making use of the reltionships derived in section 2.5. It will appear that one of the assumptions made in the derivations in this section is that the refractive index variations have a Kolmogorov-type spatial spectrum. The consequences of this assumption will be dealt with in section 2.7. Finally, section 2.8 will summarize the assumptions made in the derivation of the relationship between the signal of the LAS and the C_{n^2}.

2.5 Log-amplitude flucuations in a spherical wave

Log-amplitude flucuations in a spherical wave: first order theory

Since the light source of a LAS can be interpreted as a collection of point sources, the propagation of a *spherical* wave through a random medium needs to be analysed (rather than that of a plane wave)[5]

[5]Whether a source can be considered a *point* source depends on the ratio between the diameter of the source and the diameter of the optically most active eddies (of which the diameter depends on the distance from both the transmitter and the receiver). If the

Tatarskii (1961) derives the log-intensity fluctuations ($\overline{\chi^2}$) in a spherical wave due to the passage of that wave through a medium with random refractive index fluctuations. The full derivation will not be reproduced here, but the main steps will be shown, with emphasis on the assumptions made. Comments on the validity of the derivation and on the necessity of assumptions made in it are given by Strohbehn (1968). Lee and Harp (1969) present a different approach in which refractive index inhomogeneities are interpreted as transmission gratings. Their derivation will not be shown here, but some of their results will be alluded to.

Tatarskii starts with a scalar wave equation[6] for a wave u in an inhomogeneous medium. From the start he assumes that the wave under consideration is short, i.e. the inhomogeneities are much larger than the wavelength ($l_0 \gg \lambda$)[7]. Strohbehn (1968) shows that this assumption is mainly needed to ensure that small-angle scattering can be assumed.

In order to be able to use less stringent conditions on the magnitude of amplitude and phase fluctuations, he turns to a propagation equation for the logarithm of the wave, $\psi = \ln u$, so that the real part of ψ is the logarithm of the amplitude and imaginary part is its phase. Then ψ is decomposed into a unperturbed part and a perturbation: $\psi = \psi_0 + \psi_1$ and the refractive index is decomposed as $n = 1 + n_1$. A differential equation for ψ_1 results which is valid provided $|n_1| \ll 1$ and the variations of ψ_1 over distances of the order of λ are small. The solution of the differential equation is

$$\psi_1(\boldsymbol{r}) = \frac{k^2}{2\pi u_0(\boldsymbol{r})} \int_V n_1(\boldsymbol{r}') u_0(\boldsymbol{r}') \frac{e^{ik|\boldsymbol{r}-\boldsymbol{r}'|}}{|\boldsymbol{r}-\boldsymbol{r}'|} dV' \,, \tag{2.16}$$

where V is the volume containing refractive index inhomogeneities and k is the wavenumber of the electromagnetic radiation ($= 2\pi/\lambda$).

Then Tatarskii applies (2.16) to a spherical wave of the form $u_0(\boldsymbol{r}) = Qe^{ikr}/r$. A consequence of the assumption that $\lambda/l_0 \ll 1$ is that light is scattered in the forward direction in a very narrow cone with an aperture angle of the order λ/l_0 (see van de Hulst (1981): scattering by large particles). Then, any substantial contribution to the the integral in (2.16) is restricted to a cone with its vertex at the observation point and an aperture angle of $\theta \sim \lambda/l_0$. Inside this narrow cone the radius r can be approximated as $r \approx x + (y^2 + z^2)/2x$ and the spherical wave can approximated accordingly as

$$u_0(\boldsymbol{r}) \approx \frac{Q}{x} \exp\left(ik(x + (y^2 + z^2)/2x)\right)$$

Lee and Harp (1969) show that the assumption $\lambda/l_0 \ll 1$ is too restrictive. For $\lambda/l_0 \geq 1$ the scattered radiation does not propagate more than a few wavelengths and consequently does not cause any interference at the detector. In the region that $\lambda/l_0 = 1$ to $\lambda/l_0 \ll 1$ wide-angle scattering occurs. According to Lee and Harp (1969) this can safely be ignored for two reasons. First, a finite receiving aperture will result in a limited cone from which scattered light is collected (as opposed to an infinitely small aperture which would collect radiation from half a hemisphere). Secondly, if $\lambda \sim l_0$ the optically most active inhomogeneities will generally be larger than l_0 (for realistic path lengths) and thus the contribution of eddies of size l_0 will be neglectable (see the discussion on page on page 10 on the size of the optically most active eddies).

The next step is to express both the field of refractive index fluctuations and the fluctuations of the spherical wave in stochastic Fourier-Stieltjes integrals[8]. Analysis of (2.16) yields the relationship between the random complex amplitudes found in the Fourier-Stieltjes integrals of n ($d\nu(\kappa_2, \kappa_3, x)$) and ψ_1 ($d\phi(\kappa_2, \kappa_3, x)$). Subsequently, the spectral amplitude of the log-amplitude fluctuation ($da(\kappa_2, \kappa_3, x)$) is found from $d\phi$[9]:

$$da(\kappa_2, \kappa_3, x) = -k \int_0^L dx \sin\left(-\frac{L(L-x)(\kappa_2^2 + \kappa_3^2)}{2kx}\right) d\nu(\kappa_2 \frac{L}{x}, \kappa_3 \frac{L}{x}, x) \tag{2.17}$$

Equation (2.17) shows that variations in the log-amplitude with wave number κ are caused by refractive index fluctuations with wave numbers $\frac{L}{x}\kappa$. Thus the inhomogeneities in n at position x are magnified by

largest eddies are (much) larger than the source of radiation, the latter can be assumed to be a point source.

[6] This excludes polarization effects.

[7] This is a trivial assumption at optical wave lengths but poses a severe restriction in the case of milimeter or centimeter waves.

[8] As an example the Fourier-Stieltjes integral for the refractive index is given: $n_1(x, y, z) = \iint_{-\infty}^{\infty} \exp\left(i(\kappa_2 y + \kappa_3 z)\right) d\nu(\kappa_2, \kappa_3, x)$

[9] $da(\kappa_2, \kappa_3, x) = \frac{1}{2}(d\phi(\kappa_2, \kappa_3, x) + d\phi^*(-\kappa_2, -\kappa_3, x))$

a factor L/x. The argument of the sine in (2.17) (i.e. $L(L-x)\kappa^2/2kx$) is equal to $\pi\Lambda^2/l'^2$, where Λ is a kind of localized radius of the first Fresnel zone (i.e. $\sqrt{\lambda(L-x)}$) and l' is the size of inhomogeneities in n at the position x in the path that cause fluctuations of size l at $x = L$. Furthermore, the product $\overline{\nu(\kappa_2,\kappa_3,x_1)\nu^*(\kappa_2',\kappa_3',x_2)}$ can be expressed in the two-dimensional spectrum $F_n(\kappa_2,\kappa_3,|x_1-x_2|)$ [10].

The variance of the log-amplitude at $x = L$ and $y = z = 0$ is derived from da as

$$\overline{\chi^2}(L,0,0) = \iiint_{-\infty}^{\infty} \overline{da(\kappa_2,\kappa_3,L)da^*(\kappa_2',\kappa_3',L)}\,. \tag{2.18}$$

Combination of (2.17) and (2.18) yields a complicated six-fold integral. One simplification can be made if the turbulence is assumed to be isotropic, since then one can proceed in polar coordinates in the (κ_2,κ_3) plane (getting rid of two integrations). Another assumption is that the two-dimensional spectrum $F_n(\kappa,|x_1-x_2|)$ is unequal to zero for $\kappa|x_1-x_2| \leq 1$ only (in order to further simplify one of the integrals). The final result is the following expression for the variance of the log-amplitude variation:

$$\overline{\chi^2} = 4\pi^2k^2L\int_0^{\infty}\Phi_{nn}(\kappa)d\kappa\int_0^{\kappa}\sin^2\left(\frac{L\kappa'(\kappa-\kappa')}{2k}\right)d\kappa'\,. \tag{2.19}$$

Although this expression for $\overline{\chi^2}$ has been derived under the assumption of isotropy, Tatarskii (1961) shows that it can be applied in situations of *local* isotropy as well. Equation (2.19) is equivalent to the expression quoted by Wang *et al.* (1978) (using the substitution $x = L\kappa'/\kappa$):

$$\overline{\chi^2} = 4\pi^2k^2\int_0^{L}dx\int_0^{\infty}d\kappa\kappa\Phi_{nn}(\kappa)\sin^2\left(\frac{\kappa^2x(L-x)}{2Lk}\right)\,. \tag{2.20}$$

From the latter equation it is clear that $\overline{\chi^2}$ at $x = L$ is the combined result of the three-dimensional spectrum of the n-fluctuations and a function that depends on the position in the path, the wave number of the turbulence and the wave number of the light used. The argument of the sine in (2.20) equals $\pi\Lambda^2/l_\kappa$, i.e. π times the square of the ratio between the localized radius of the first Fresnel zone (see on the current page) and the size of the turbulent eddy under consideratio (l_κ).

Recalling that the structure function D_{nn} and the spectral density Φ_{nn} are related (see equation (2.5)), (2.20) can be rewritten as:

$$\overline{\chi^2} = \int_0^{L}dxC_{n^2}(x)W(x)\,, \tag{2.21}$$

where $W(x)$ is a weighting function:

$$W(x) = 4\pi^2k^2\int_0^{\infty}d\kappa\kappa\Phi_{nn}(\kappa)\sin^2\left(\frac{\kappa^2x(L-x)}{2Lk}\right)\,, \tag{2.22}$$

and C_{n^2} is the structure function parameter of the refractive index, which may be –smoothly– dependent on x since only *local* isotropy is assumed in the derivation. The function $W(x)$ depends on the exact form of the spectral density (Φ_{nn}) and on the ratio $\pi\Lambda^2/l_\kappa$. Tatarskii shows that for the situation where $\sqrt{\lambda L} \ll l_0$ the weighting function $W(x)$ is proportional to L^3 and to an integral of the spectral density Φ_{nn}, and is independent of the optical wave number. On the other hand, for $\sqrt{\lambda L} \gg l_0$ he shows that $W(x) \sim k^{7/6}L^{11/6}$, if a Kolmogorov spectrum is assumed: $\Phi_{nn}(\kappa) \sim \kappa^{-11/3}$. The dependence of the weighting function upon the position in the path then becomes $W(x) \sim \left(\frac{x}{L}(1-\frac{x}{L})\right)^{5/6}$. Carrying out the integration, yields the following expression for $\overline{\chi^2}$ (Wang *et al.*, 1978):

$$\overline{\chi^2} = 0.124k^{7/6}L^{11/6}\overline{C}_{n^2}\,, \tag{2.23}$$

[10] It should be noted that the fi eld of χ is not statistically homogeneous in the plane $x = L$, at which the current analysis is looking, but on the sphere $r = L$

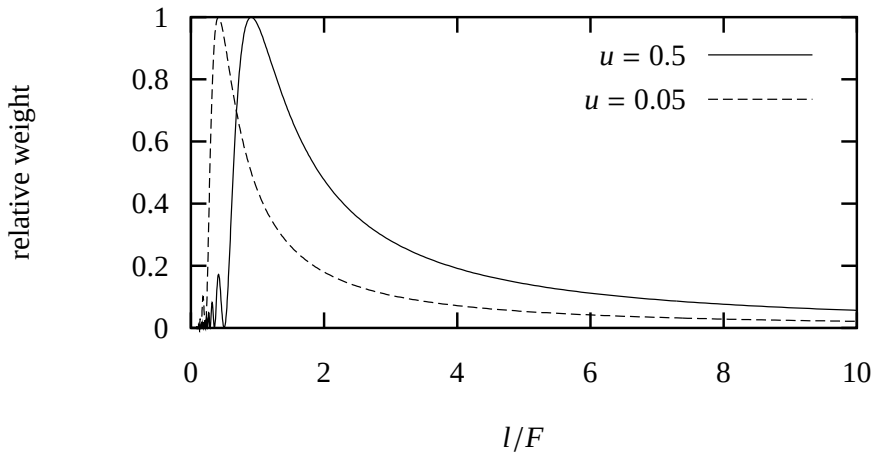

Figure 2.1: Value of the integrand in (2.22) as a function of the size of the inhomogeneities l. The eddy size l has been normalized by the diameter of the first Fresnel zone and the maximum of the weighting function has been normalized to 1. The curve given is for both $u = 0.5$ and $u = 0.05$. The maximum of the weighting function for $u = 0.5$ is located at $l/\sqrt{\lambda L} \approx 0.9$.

where $\overline{C}_{n^2}$ is a path averaged value of C_{n^2}, weighted with the weighting function (2.22). With the use of the weighting function (2.22) the scale of the optically most active inhomogeneities can be deduced (assuming a form for $\Phi_{nn}(\kappa)$). To do this, the maximum of

$$\kappa\Phi_{nn}(\kappa)\sin^2\left(\frac{\kappa^2 u(1-u)F^2}{4\pi}\right)$$

has to be found, where u is the relative position in the path x/L and F is the size of the first Fresnel zone ($\sqrt{\lambda L}$). The first (and highest) maximum of this function occurs at $\kappa^2 u(1-u)F^2/4\pi \approx 1$, so that the length-scale of the most effective eddies is $l = \sqrt{\pi u(1-u)}F$. Thus the optically most active eddies are of the order of the diameter of the first Fresnel zone in the center of the path and decrease in size towards the transmitter and the receiver. Figure 2.1 shows the value of the integrand in (2.22) as a function of the size of the inhomogeneity: $l = 2\pi/\kappa$. It can be seen that for $l/F > 1$ the integrand decreases only gradually. This would suggest that large inhomogeneities make a significant contribution to the log-amplitude variance. However, in order to judge the real contribution of eddies of a given size, the integrand should be studied as it appears in (2.22), i.e. as a function of κ (or l^{-1}, rather than l. This is shown in figure 2.2.

2.5.1 Log-intensity fluctuations in a spherical wave in strong turbulence

The expressions shown in the previous section where derived for first-order scattering, i.e. a scattered wave arriving at the detector is assumed to have been scattered only once. In strong turbulence $\overline{\chi^2}$ becomes saturated: an increase of C_{n^2} no longer results in an increase of $\overline{\chi^2}$ and the proportionality between the two is lost. Saturation occurs at $\overline{\chi^2} \approx 0.3$ (Clifford *et al.*, 1974). Thus for a given optical wave length and a given range of C_{n^2} saturation poses a limit on the path length L.

Clifford *et al.* (1974) explain the lack of increase of $\overline{\chi^2}$ with C_{n^2} as follows. A given inhomogeneity in n at position x causes an intensity fluctuation at the detector. The inhomogeneity is interpreted as a lens that focuses light on a screen at $x = L$ (but note that the detector at $x = L$ is a *point*-detector. In strong turbulence the wave front that illuminates the inhomogeneity at x is no longer spherical, since it was distorted by previous inhomogeneities.

Irregularities in the wave front with a scale *less* than the size of the lens will result in a pattern at the screen at $x = L$ that is a smeared version of the pattern which would appear in the case of a pure spherical

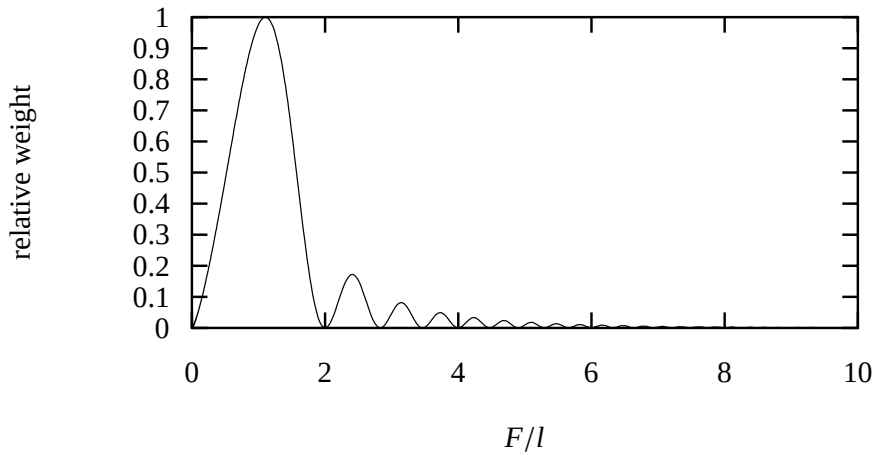

Figure 2.2: Contribution of different eddy sizes to the integrand in (2.22). The eddy size is given as F/l in order that the curve represents the contribution of a given size to the total log-amplitude variance. The maximum of the weighting function has been normalized to 1. The curve given is for $u = 0.5$. The maximum of the weighting function for $u = 0.5$ is located at $\sqrt{\lambda L}/l \approx 1.1$.

wave[11] The smearing of the image at the position of the detector will result in a decrease of the variance of the log amplitude. Besides, the small scale distortions of the wave front have a time scale which is shorter than that of the Fresnel-zone-sized eddy under consideration. Thus the spot at the screen at $x = L$ will change in detail continuously. Irregularities in the wave front with a scale *larger* than the *n*-inhomogeneity will result in a tilt of the wave and subsequent displacement (but not distortion) of the spot on the screen. Clifford *et al.* suggest that the effect of extra scattering between the lens under consideration and the receiver is identical to the effect of scattering between transmitter and lens.

Clifford *et al.* (1974) derive an expression for the log-amplitude variance[12] resulting from the passage of a spherical wave through a strongly turbulent field of refractive index fluctuations. The main steps in the derivation can be summarized as follows:

a. The starting point is an expression for the irradiance profile at a given position due to an aperture at another position that is illuminated by a random optical field.

b. Each Fourier component of the refractive index field is interpreted as a physical aperture that is illuminated by a turbulence-distorted optical field and that transmits this field through a turbulent medium to a screen at $x = L$.

c. The log-amplitude fluctuations at $x = L$ are assumed to be described by a convolution of the covariance of the log-amplitude fluctuations resulting from first order scattering and the irradiance profile function referred to under point **a**. In the spatial frequency domain this convolution can be replaced by a multiplication of the first order log-amplitude spectrum with a spectral filter function (the two-dimensional Fourier transform of the function referred to under **a**).

d. In order to eliminate the effect of tilting and retain only the smearing effect a low wavenumber cut-off is used for the filter function mentioned under **c**. This cut-off is assumed to be proportional to the wave number of the *n*-inhomogeneity (i.e. the lens) under consideration.

[11] The smearing of the image can be understood as follows. The spot at the screen at $x = L$ is composed of contributions originating from all point of the lens (i.e. the *n*-inhomogeneity). At the lens the irregularities in the wave front can be interpreted as uncertainties –or errors– in the exact position of the point source. This uncertainty results in an uncertainty in the position at the screen of each contribution to the spot.

[12] In fact they derive an expression for the covariance function in the plane $x = L$, but this spatial information is not relevant for the present discussion. Here the covariance at zero lag will be used, i.e. the variance.

e. The turbulence is assumed to be homogeneous and isotropic along the entire path.

The resulting expression for the log-amplitude variance at $x = L$ is:

$$\overline{\chi^2} = 2.94\sigma_{\chi,0}^2 \int_0^1 du\,(u(1-u))^{5/6} \int_0^\infty g(u,y)dy\,, \tag{2.24}$$

where

$$g(u,y) = y^{-11/6}\sin^2(y)\exp\left(-\sigma_{\chi,0}^2\,(u(1-u))^{5/6}\,f(y)\right)\,,$$
$$f(y) = 7.02y^{5/6}\int_{0.7y}^\infty d\xi\xi^{-8/3}\,(1-J_0(\xi))\,,$$
$$y = \frac{\kappa^2 u(1-u)L}{2k} = \frac{\kappa^2 u(1-u)F^2}{4\pi}\,,$$

where F is the diameter of the first Fresnel zone and $\sigma_{\chi,0}^2$ is the log-amplitude variance resulting from first order theory (i.e. (2.23)). The difference between the above expression for $\overline{\chi^2}$ and the first order approximation (2.23) is an exponential term, involving $\sigma_{\chi,0}^2$. This term reduces to 1 for low turbulence situations (i.e. low C_{n^2}). Clifford *et al.* claim that (2.24) reduces asymptotically to the first-order result for $\sigma_{\chi,0}^2 \leq 0.3$. However, numerical evaluation of the integrals shows that for $\sigma_{\chi,0}^2 = 0.3$ the difference between (2.24) and (2.23) is still of the order of 15%.

The structure of equation (2.24) can be interpreted as follows. The term in the inner integral describes the contributions of the different wave numbers to the log-intensity variance. The term in the outer integral (including the inner integral) describe the contribution of n-variations at a given position in the path to the total log-intensity variance. It is this outer integral which is often called the *weighting function*.

2.6 The Large Aperture Scintillometer

Wang *et al.* (1978) observe two problems in the application of scintillometers for the estimation of the structure function parameter of n:

- The linear relationship between $\overline{\chi^2}$ and C_{n^2} is valid only for very weak turbulence (as shown in the previous section). In strong turbulence the $\overline{\chi^2}$ becomes saturated: an increase of C_{n^2} no longer results in an increase of $\overline{\chi^2}$ and the proportionality between the two is lost. Thus for a given optical wave length and a given range of C_{n^2} saturation poses a limit on the path length L.
- For short path lengths the weighting function (and thus the relationship between $\overline{\chi^2}$ and C_{n^2} will depend on the exact shape of the spectrum Φ_{nn} at high wave numbers. This in turn depends on the micro-scale l_0 which is —in general— unknown.

Ochs *et al.* (1976) conclude that both problems can be circumvented by using a scintillometer that does not observe the Fresnel-zone-sized eddies. Such scintillometer is one with a transmitter and receiver that are both spatially incoherent and have a diameter that is larger than the first Fresnel zone. The spatial incoherence is needed in order to prevent small eddies near the transmitter from causing intensity fluctuations at the receiver with a size of the order of the receiver. This so-called large aperture scintillometer (LAS) will be sensitive to refractive index inhomogeneities with a size of the order of the transmitter and receiver aperture diameter (see below). Provided that this is larger than the inner scale, the calibration of the LAS will not depend on the exact shape of the spectrum Φ_{nn} at high wave numbers.

In the forthcoming sections first an expression for the log-amplitude variance as measured by the LAS will be derived. Subsequently, the conditions to prevent saturation will be discussed. And finally, the relationship between $\overline{\chi^2}$ and C_{n^2} for the LAS will be shown.

2.6.1 The log-amplitude variance for the LAS

The expression for the log-amplitude fluctuations at the receiver of a LAS is essentially a small modification of the expression for the scintillometer with infinitely small transmitter and receiver diameters. In (2.24)

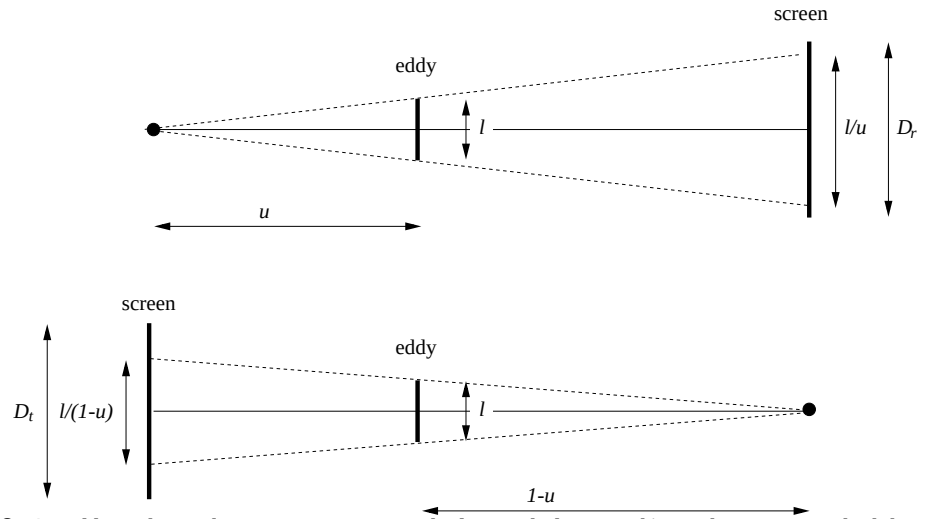

Figure 2.3: An eddy with size l, at position u casts a shadow with diameter l/u on the receiver, which has a diameter D_r. The shadow on the transmitter is $l/(1-u)$ in size.

the function $g(u,y)$ has to be replaced by $g'(u,y)$, which equals:

$$g'(u,y) = g(u,y)\left(\frac{2J_1(\sqrt{y/y_r})}{\sqrt{y/y_r}}\right)^2\left(\frac{2J_1(\sqrt{y/y_t})}{\sqrt{y/y_t}}\right)^2 = g(u,y)A, \tag{2.25}$$

where

$$y_r = \frac{1-u}{u}\frac{1}{\alpha_r^2\pi}\ ,$$

$$y_t = \frac{u}{1-u}\frac{1}{\alpha_t^2\pi}\ ,$$

y as defined below equation (2.24), and α_t and α_r are the diameters of the transmitter and receiver, expressed in Fresnel zone diameters. The physical interpretation of the terms $\sqrt{y/y_t}$ and $\sqrt{y/y_r}$ can be found by use of the definitions of y, y_r and y_t:

$$\sqrt{y/y_r} = \sqrt{\frac{1}{4}\kappa^2u^2\alpha_r^2L\lambda} = \frac{1}{2}\kappa u D_r\ , \tag{2.26a}$$

$$\sqrt{y/y_t} = \sqrt{\frac{1}{4}\kappa^2(1-u)^2\alpha_t^2L\lambda} = \frac{1}{2}\kappa(1-u)D_t\ , \tag{2.26b}$$

where D_r and D_t are the —physical— diameters of receiver and transmitter, respectively. In the sequel both diameters are assumed to be equal. An eddy with wave number $\frac{1}{2}\kappa$ has a size of π/κ. Consider this eddy to be located at the relative position between transmitter and receiver u. When illuminated from the transmitter with a spherical wave it will cast a shadow with a diameter $\pi/(\kappa u)$ at the receiver. Thus $\sqrt{y/y_r}$ is π times the ratio between the diameter of the receiver and the diameter of the shadow of an eddy with wave number κ at position u. Analogously, $\sqrt{y/y_t}$ is π times the ratio between the transmitter diameter and the image at the transmitter of an eddy with wave number κ, located at u and illuminated by a point source at the receiver. Thus, for a given transmitter or receiver diameter, and a given position in the path, $\sqrt{y/y_t}$ and $\sqrt{y/y_r}$ are inversely proportional to the size of the n-inhomogeneity under consideration (see figure 2.3).

The next step is to consider the dependence of the factor A in (2.25) on y, y_r and y_t. The function $(2J_1(x)/x)^2$ equals 1 for $x = 0$, decreases towards 0 for $x \lesssim 3.8$ (say x_{max}), and oscillates between zero and a quickly decreasing upper value for $x > 3.8$ (the second maximum is of the order of 0.02). Physically, this implies that the factor in A involving y/y_r is non-zero only for eddies that cast a shadow on the receiver that is of the order of, or much larger than, the receiver[13]. In the same way the part of A involving y/y_t is

[13]Remember that $\sqrt{y/y_r}$ is π times the ratio between the transmitter diameter and the eddy size

non-zero only for eddies that cast large shadows on the transmitter. An eddy that is close to the transmitter will cast a *large* shadow on the receiver, but a *small* shadow on the transmitter. Consequently, the two factors that make up A are each others mirror images around $u = 0.5$. A is unequal to zero for eddies with a size equal to or larger than the aperture diameter, since only for these eddies the shadows on both receiver and transmitter are larger than the aperture diameter.

2.6.2 Prevention of saturation

Thus it has been shown that a large aperture scintillometer is not sensitive to eddies with a size smaller than the aperture diameter (as was qualitatively required in order to prevent saturation). In order to make a quantitative statement on the occurrence or absence of saturation the behaviour of the function $g'(u,y)$ needs to be explored. In terms of this function, saturation can be prevented in two ways:

a. The argument of the exponential function is small (i.e. $F(y)$ is small given that $\sigma^2_{\chi,0}$ may be large).

b. The factor A is small for those values of y for which $\sigma^2_{\chi,0}$ and $F(y)$ are not small.

In order to judge the condition mentioned under **a**, some knowledge of the function $F(y)$ is needed. $F(y)$ has two limiting forms, viz. $7.9y^{5/6}$ for $y < 1$ and $7.9y^{-5/6}$ for $y > 1$ (Wang *et al.*, 1978), so that $F(y)$ is small for $y \ll 1$ and $y \gg 1$. Thus condition **b** needs to take care of the intermediate region of where y is of the order of 1. Above it has been shown that the factor A is non-zero only for eddies that are large relative to the scintillometer aperture diameter (i.e. have a low wave number). This shuts off the region $\sqrt{y/y_{t,r}} \gg x_{max}$. Now it depends on the variables that constitute y_t and y_r whether this will shut off the region where $y \approx 1$. There are two options to eliminatre the influence of $\sigma^2_{\chi,0}$ on $\overline{\chi^2}$ in this region.

a. The upper limit of the relevant region of integration in the inner integral in (2.24), y_{max}, is much less than one;

b. The upper limit of integration, y_{max} is of the order of one, but the decrease of the factor A cancels the influence of the exponential term in $g(u,y)$.

The maximum value of y, y_{max}, corresponding to x_{max} is (recalling the definitions of y_r and y_t, and taking $\alpha_t = \alpha_r$):

$$y_{max} = \min\left(x^2_{max}\frac{1-u}{u}\frac{1}{\alpha^2\pi}, x^2_{max}\frac{u}{1-u}\frac{1}{\alpha^2\pi}\right) \tag{2.27}$$

The minimum of the factors involving u is 1 or less, so that y_{max} is at most $x^2_{max}\pi^{-1}\alpha^{-2}$. In order for y_{max} to be much less than 1 (situation a), $\alpha \gg x_{max}\sqrt{\pi^{-1}} \approx 2.1$. However, if this $y_{max} < 1$ rather than $y_{max} \ll 1$ situation b is applicable and condition **a** and **b** need to be taken into account simultaneously. For this analysis it is convenient that $(2J_1(x)/x)^2$ can be approximated as $\exp(-\frac{1}{4}x^2)$ for $x < 1$. Thus the product of A and the exponential term in $g(u,y)$ becomes:

$$\exp\left(-\sigma^2_{\chi,0}(u(1-u))^{5/6}F(y) - \frac{1}{4}\left(\frac{y}{y_t}+\frac{y}{y_r}\right)\right) .$$

In order for $\sigma^2_{\chi,0}$ to have negligible influence on the value of this exponential term it should be required that:

$$\begin{aligned}\sigma^2_{\chi,0}(u(1-u))^{5/6}F(y) &\ll \frac{1}{4}\left(\frac{y}{y_t}+\frac{y}{y_r}\right)\\ &\ll \frac{1}{4}\alpha^2\pi\frac{\kappa^2 L}{2k}\left((1-u)^2+u^2\right)\end{aligned}$$

Setting $(u(1-u))$ to 0.25 (its maximum, worst case, value), $u^2+(1-u)^2$ to 0.5 (its minimum), and replacing $F(y)$ by its approximation for $y < 1$ (see above), the following inequality results:

$$\frac{1}{4}\sigma^2_{\chi,0}7.9y^{5/6} \ll \frac{1}{4}y\pi\alpha^2 .$$

Since $y < 1$, the difference between y and $y^{5/6}$ is small, so that finally:

$$\alpha \gg 1.6\sqrt{\sigma_{\chi,0}^2}\,, \tag{2.28}$$

which is qualitatively equivalent to, but more stringent than, the limit given by Wang *et al.* (1978): $\alpha > 0.98(\sigma_{\chi,0}^2)^{3/5}$.

Relationship between $\overline{\chi^2}$ and C_{n^2}

If the diameter of the LAS is sufficiently large in order to prevent saturation, the expression for the log-amplitude variance is:

$$\overline{\chi^2} = 2.94\sigma_{\chi,0}^2 \int_0^1 du\,(u(1-u))^{5/6} \int_0^\infty dy y^{-11/6} \sin^2 y \left(\frac{2J_1(\sqrt{y/y_r})}{\sqrt{y/y_r}}\right)^2 \left(\frac{2J_1(\sqrt{y/y_t})}{\sqrt{y/y_t}}\right)^2\,, \tag{2.29}$$

Above it has been shown that the upper limit of the relevant region of integration in the inner integral in (2.29), y_{max}, is proportional to α^{-2} (i.e. $y_{max} = \beta\alpha^{-2}$, see equation (2.27)). Furthermore, $y_{max} < 1$ and for the relevant region of integration it was ensured that the exponential term was approximately equal to 1. Thus the double integral in (2.29) can be simplified as follows:

$$\begin{aligned}\int_0^1 du(u(1-u))^{5/6} \int_0^\infty dy g'(u,y) &\approx \int_0^1 du(u(1-u))^{5/6} \int_0^{\beta\alpha^{-2}} dy g(u,y) \\ &= \int_0^1 du(u(1-u))^{5/6} \int_0^{\beta\alpha^{-2}} dy y^{-11/6} \sin^2 y\end{aligned} \tag{2.30}$$

For small y, $\sin y$ can be approximated as y, so the double integral becomes:

$$\int_0^1 du(u(1-u))^{5/6} \int_0^{\beta\alpha^{-2}} y^{1/6} dy = \int_0^1 du \int_0^{\beta\alpha^{-2}} (u(1-u))^{5/6} \left(\frac{\kappa^2 u(1-u)F^2}{4\pi}\right)^{1/6} dy$$

Changing the integration variable to $x = \kappa^2 F^2/4\pi$ the integrals can be evaluated:

$$\begin{aligned}\int_0^1 du \int_0^{\beta\alpha^{-2}/u(1-u)} (u(1-u))x^{1/6} dx &= \frac{6}{7}\int_0^1 \left|u(1-u)x^{7/6}\right|_0^{\beta\alpha^{-2}/u(1-u)} du \\ &= \frac{6}{7}\beta^{7/6}\alpha^{-7/3}\int_0^1 (u(1-u))^{1/6} du \\ &= \frac{6}{7}\beta^{7/6}\alpha^{-7/3}\left|\frac{6}{7}u^{7/6} - \frac{6}{8}u^{8/6}\right|_0^1 \\ &= \frac{6}{7}\left(\frac{6}{7} - \frac{6}{8}\right)\beta^{7/6}\alpha^{-7/3}\end{aligned}$$

The value of β can be found from comparison of the latter expression with a numerical evaluation of the full integral (the double integral in (2.29)). β turns out to be 0.808 approximately and the value only depends on the ratio between the diameters of transmitter and receiver (which are assumed to be equal here). Combination of the latter expression for the double integral with (2.29) gives together with expansion of $\sigma_{\chi,0}$ (equation (2.23)), and conversion of the normalized aperture diameter α to a physical diameter $D = \alpha\sqrt{\lambda L}$:

$$\begin{aligned}\overline{\chi^2} &= 2.94\sigma_{\chi,0}^2 \frac{6}{7}\left(\frac{6}{7} - \frac{6}{8}\right)\beta^{7/6}\alpha^{-7/3} \\ &= 0.211\sigma_{\chi,0}^2\alpha^{-7/3} \\ &= 0.0261k^{7/6}L^{11/6}\alpha^{-7/3}\overline{C_{n^2}} \\ &= 0.0261(2\pi)^{7/6}D^{-7/3}L^3\overline{C_{n^2}}\end{aligned}$$

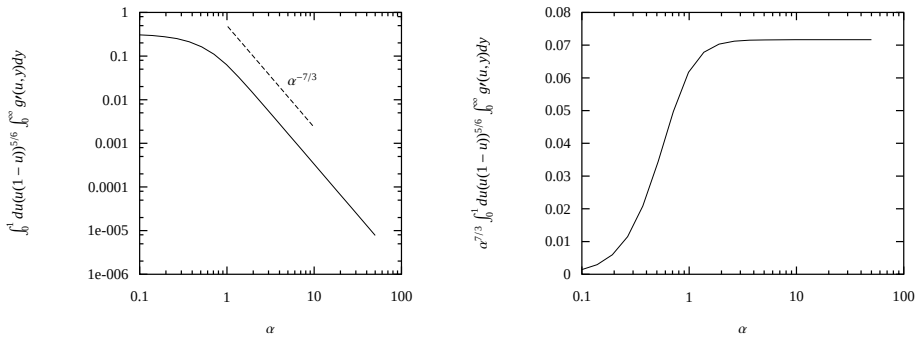

Figure 2.4: Dependence of double integral $Ag(u,y)$ in equation (2.25) on diameter of receiver and transmitter, α ($= D/\sqrt{L\lambda}$). For small diameters the integral is no longer proportional to $\alpha^{-7/3}$. Left: $Ag(u,y)$ as a function of α. Right: a compensated plot of $Ag(u,y)$, i.e. $\alpha^{7/3}Ag(u,y)$ as a function of α.

This finally leads to the expression for $\overline{\chi^2}$:

$$\overline{\chi^2} = 0.223D^{-7/3}L^3\overline{C_{n^2}} \tag{2.31}$$

This is in accordance with the expression found by Wang *et al.* (1978). It should be noted here that proportionality of the double integral in (2.29) to $\alpha^{-7/3}$ is valid only for sufficiently large α. This is shown in figure 2.4. The cause of this deviation is that if α is not sufficiently large, the integration in (2.30) is carried out over a range of y where the assumption $\sin y = y$ no longer holds .

The relative contribution of n-variations at different positions in the path to the total log-intensity variance at the detector is shown in figure 2.5. It is clear that $\alpha > 2$ ($\alpha = D/F$) in order for the calibration of the LAS to be independent of the beam diameter (see also Hill and Ochs, 1978)

2.6.3 Relationship between C_{n^2} and the signal of the LAS

The LAS uses a square law detector and thus measures the intensity of the radiation, I, rather than the amplitude, A. The intensity of electromagnetic radiation is proportional to the amplitude squared (Jenkins and White, 1976):

$$I \sim A^2 ,$$

and consequently the log-intensity, $\log I$ is proportional to the 2 times the log amplitude χ and the the variance of $\log I$ is equal to 4 times the log amplitude variance:

$$\overline{(\log I)'} = 4\overline{\chi^2} . \tag{2.32}$$

Thus equation (2.31) becomes:

$$\overline{(\log I)'} = 0.892D^{-7/3}L^3\overline{C_{n^2}} , \tag{2.33}$$

which can be inverted to obtain $\overline{C_{n^2}}$ as a function of the LAS output:

$$\overline{C_{n^2}} = 1.12D^{7/3}L^{-3}\overline{(\log I)'} , \tag{2.34}$$

2.6.4 The scale of n-inhomogeneities causing the intensity fluctuations

In section 2.5 it was observed that for infinitely small transmitter and receiver diameters the size of the optically most active inhomogeneities is of the order of the diameter of the first Fresnel zone (in the centre of the path). The log-amplitude variance is mainly produced by eddies ranging in size from 0.5 to 5 times F.

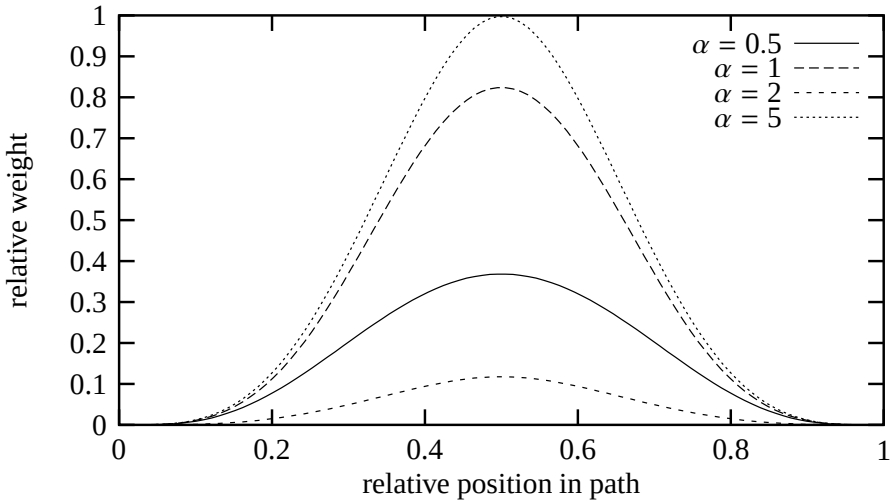

Figure 2.5: Relative contribution of n-variations at different positions in path to the log-intensity variance at the detector. The weighting functions have been multiplied with $\alpha^{7/3}$ in order to compensate for the dependence of the $\overline{\chi^2}$-C_{n^2} relationship on D (see (2.31)). The maximum of the weighting function for $\alpha \rightarrow \infty$ has been used to normalize the weighting functions.

In order to determine the size of the most active inhomogeneities in case of the LAS the integrand of the inner integral in (2.29) needs to be examined (note that $dy \sim \kappa d\kappa$). In section 2.6.1 it was observed that the effect of the factor A (the term involving the diameters of transmitter and receiver, see equation (2.25)) is to filter out log-amplitude fluctuations that are due to inhomogeneities that are smaller than the aperture diameter of the LAS. Thus as long as the aperture diameter is larger than the diameter of the first Fresnel zone ($\alpha > 1$) the strongest amplitude fluctuations (due to inhomogeneities of size F, see section 2.5, on page 10) are filtered out. Consequently, the lower limit of the size of optically active inhomogeneities, as well as the size of the *most* active ones is determined by the aperture diameter. (the first zero of A in terms of y is proportional to α^{-2} and $l \sim \kappa^{-1} \sim \sqrt{y^{-1}}$). If $\alpha < 1$ the peak in $\kappa g(u, y)$ determines the size of the optically most active eddies (which have a size $l \sim F$). For inhomogeneities that are larger than the aperture diameter the function A equals 1 and the contribution of the eddies to the log-amplitude variance is determined by the function $g(u, y)$. The interplay between the functions A and $g(u, y)$ is shown in figure 2.6.

Figure 2.7(a) shows the value of the integrand in (2.29) as a function of the size of the inhomogeneity that causes the amplitude fluctuation. The optically most active inhomogeneities have a size of 1.4 times D. For smaller eddies the contribution to the log-amplitude variances falls off rapidly. The larger eddies on the other hand show significant contributions for sizes up to 10 D and larger.

As commented on in section 2.5, a plot of the integrand versus the size of the inhomogeneity does not give a correct indication of the relative importance of the given eddy size in producing log-amplitude variations at the detector, since the integrand is stated in terms of κ (or $y \sim \kappa^2$). Therefore figure 2.7(b) gives the integrand versus D/l ($\sim D\kappa$). From this figure it is clear that all inhomogeneities with sizes $> 1.4D$ give a contribution to $\overline{\chi^2}$ that is of the same order as all inhomogeneities with $l < 1.4D$.

2.7 The effect of deviations from a Kolmogorov spectrum

Up to this point the spectral density function of n has been assumed to be described by a Kolmogorov-type spectrum throughout the range of wave numbers describing n-inhomogeneities that cause relevant log-amplitude fluctuations. This spectral density function is $\Phi_{nn}(\kappa) \sim \kappa^{-11/3}$. However, in section 2.3 it was observed that the spectral density function of a turbulent field is described by $\Phi_{nn}(\kappa) \sim \kappa^{-11/3}$ for $l_0 \ll \kappa \ll \mathcal{L}_0$ only.

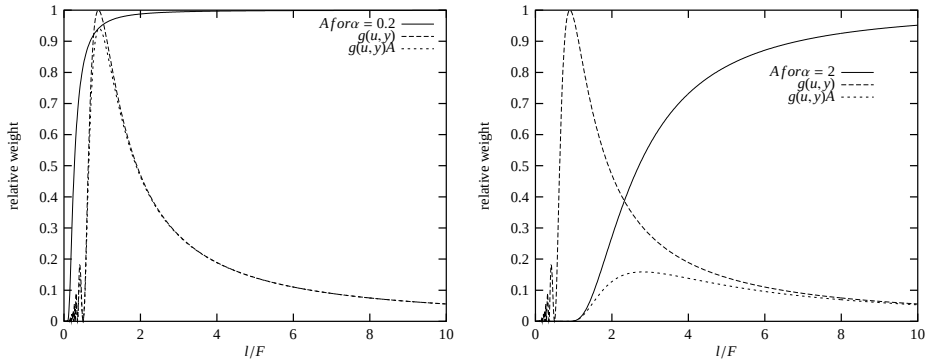

Figure 2.6: Illustration of the effect of finite apertures on the scale of optically active refractive index inhomogeneities. Plotted is the integrand of (2.24): $\kappa g'(u,y)$ ($g(u,y)$ is replaced by $g'(u,y)$ since the finite aperture is considered; in terms of wave numbers the integrand is $\kappa g'(u,y)$, since $dy = \kappa d\kappa$). Also shown are the constituent parts of the integrand: $\kappa g(u,y)$ and A. It is assumed that no saturation occurs: the exponential term (2.24) is set to 1. The factor A does depend on the aperture and the position of its first zero is proportional to α. Left: weighting function for $\alpha = 0.2$ (a small aperture), right: $\alpha = 2$ (corresponding to $L \approx 5000m$ when $\lambda = 0.93\mu m$ and $D = 0.15m$). For both figures u was set to 0.5, and the graph was normalized to have a maximum value of 1.

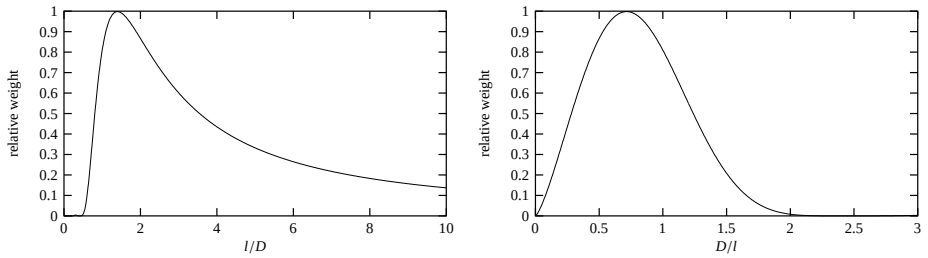

(a) (b)

Figure 2.7: The integrand in (2.29) The eddy size l has been normalized by the aperture diameter and the maximum of the weighting function has been normalized to 1. The curve given is for $u = 0.5$ and $\alpha = 5$ but the shape of the curve is rather insensitive to both u and α (for $\alpha > 1$). Graph (a) shows the integrand as a function of l/D (the maximum is located at $l/D \approx 1.4$). Graph (b): integrand as a function of D/l.

2.7.1 The effect of the inner scale

In the framework of scintillometry mainly two ways are used to describe the high wave number part of the spectral density:

- The Tatarski spectrum (Tatarski (1967), cited by Strohbehn (1968)) in which the damping of fluctuations at high wave numbers is described with an exponential :

$$\Phi_{nn}(\kappa) = 0.033 C_{n^2} \kappa^{-11/3} \exp(-\kappa^2/\kappa_m^2) \,, \tag{2.35}$$

  where $\kappa_m = 5.92/l_0$.
- For scalars with a Prandtl number less than 1, the spectral density function exhibits a 'bump' in the so-called convective-viscous region (velocity fluctuations are affected by viscosity, whereas scalar fluctuations are still unaffected by molecular diffusion). In this region the spectral density has a κ^{-3} dependency[14]. Hill (1978*a*) shows a number of models that describe this bump. The simplest model for the one-dimensional spectrum F_{nn} can be converted to a three-dimensional spectrum (with $\Phi_{nn}(\kappa) = -\frac{1}{2\pi\kappa}\frac{\partial}{\partial\kappa}F_{nn}(\kappa)$, under the constraint that in the inertial subrange the spectrum equals the Tatarski spectrum):

$$\begin{aligned}\Phi_{nn}(\kappa) = &- 0.033\frac{3}{10} C_{n^2}\kappa^{-11/3} \exp\left(-A(\frac{3}{2}y^{4/3} + y^2)\right) \\ &\left[-\frac{5}{3}(1+y^{2/3}) + \frac{2}{3}y^{2/3} - 2Ay(1+y^{2/3})(y^{1/3}+y)\right]\end{aligned} \tag{2.36}$$

  with $y = \frac{\kappa}{\kappa_d}Q^{3/2}$, $A \equiv \beta Q^{-2} Pr^{-1}$, $\kappa_d = 2\pi/l_0$, β is the Obukhov-Corrsin constant ($\approx 0.55 - 0.72$, see Hill (1978*a*)), and Q is a free parameter, Pr is the Prandtl number and χ is the dissipation of the scalar variance. Note that the 'bump' spectrum includes the exponential decrease at high wave numbers that is characteristic of the Tatarski spectrum. One deficiency of (2.36) is that the bump is too wide and the spectrum does not collapse to a Kolmogorov spectrum quickly enough when $\kappa \to 0$.
- The second model presented by Hill is:

$$\Phi_{nn}(\kappa) = 0.033 C_{n^2}\beta \left(\frac{\kappa^*}{\kappa_d}\right)^{-5/3} \left(-\frac{1}{2\pi\kappa}\frac{\partial F_{nn}(\kappa)}{\partial\kappa}\right)$$

  with:

$$\begin{aligned}F_{nn} = &\left(\frac{\kappa}{\kappa^*}\right)^{-4/3} (2\cosh(az^*))^{1/3a} \\ &\exp\left(-2\beta\left(\frac{\kappa^*}{\kappa_d}\right)^{4/3} Pr^{-1} \int_{-\infty}^{z^*} \exp(5w/3)\,(2\cosh(aw))^{1/3a}\, dw\right)\end{aligned} \tag{2.37}$$

  where κ^* is a transitional wavenumber (wavenumber where one-dimensional spectrum on log-log plot has slope $-\frac{4}{3}$), $z^* \equiv ln\frac{\kappa}{\kappa^*}$, and a and $\frac{\kappa^*}{\kappa_d}$ need to be determined from experiment (here the values 1.7 and 0.073 will be used).
- The fourth model spectrum presented by Hill (the third spectrum not being dealt with here) can be described with the following differential equation:

$$\frac{d}{d\kappa}H(\kappa)\frac{d}{d\kappa}\Phi_{nn} = \frac{2}{Pr}\kappa^4\Phi_{nn}(\kappa)$$

[14] Hill (1978*a*) deals with scalar spectra, in particular with the temperature spectrum. In the optical wavelength range under consideration (around 0.93 μm), the refractive index mainly depends on temperature and to a lesser extent on humidity (see section 3). Since the Schmidt number for humidity is close to the Prandtl number for heat, the results based on temperature spectra will be valid for the refractive index as well, in good approximation (see Hill, 1978*b*). Therefore, in the sequel Φ_{nn} will be used, where in principle the spectral density of a single scalar should have been used.

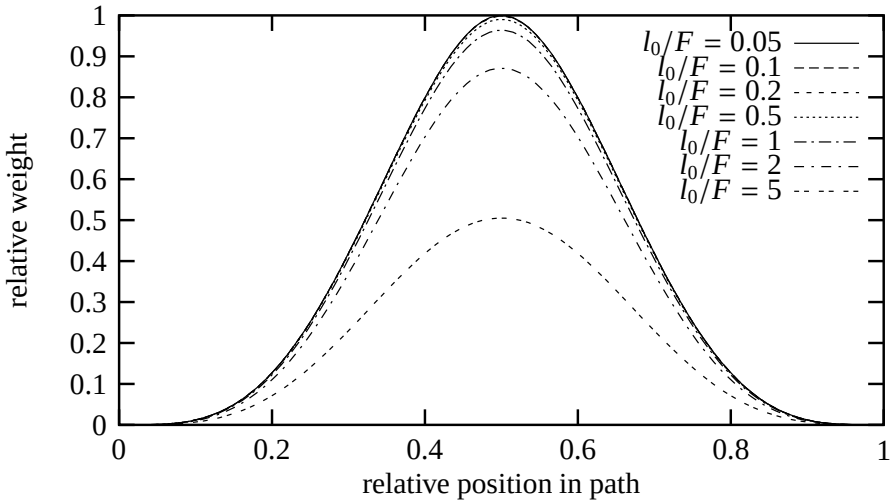

Figure 2.8: Dependence of weighting function on micro scale (using Tatarski's spectrum ((2.35)). The weighting functions have been normalized such that the maximum of the weighting function at infinitely small l_0 is 1. Furthermore, $F = 0.03m$ and $D = 0.15m$ (i.e. $\alpha = 5$). The lines for $l_0/F = 0.1$ and 0.05 coincide.

with:

$$H(\kappa) = \frac{3}{11}\beta^{-1}\eta^{-4/3}\kappa^{14/3}\left[\left(\frac{\kappa}{\kappa^{\dagger}}\right)^{2b} + 1\right]^{-1/(3b)} \tag{2.38}$$

where $\kappa^{\dagger} = 0.072/\eta$, η is the Kolmogorov micro scale and $b = 1.9$. This fourth model spectrum fits experimental spectra best (see Hill, 1978*a*).

Figure 2.8 shows the effect of the the micro scale (described with the Tatarski spectrum) on the path weighting function (compare to figure 2.5). It can be seen that for micro scales of the order of about $1/50$ of the beam diameter there is no effect of the micro scale on the weighting function. In order to explore this dependence of the calibration of the LAS on the beam diameter, figure 2.9 shows the dependence of the calibration factor of the LAS (i.e. the integral of the weighting function over $0 < u < 1$) for various ratios of l_0/D and various assumed shapes of the refractive index spectrum. One can see that indeed for $l_0/D > 0.02$ the relative calibration factor deviates from 1. However, where the Tatarski spectrum predicts a monotone decrease of the calibration factor with increasing l_0, the Hill spectra suggest a small decrease, followed by a large –local– increase of the calibration factor with increasing l_0.

Hill and Ochs (1978) already studied the effect of the 'bump' in the temperature spectrum (and consequently in the refractive index spectrum) on the validity of the calibration of the LAS (i.e. equation (2.29)). They conclude that the aperture diameter should be at least 30 times l_0 in order for the calibration to be independent of l_0. This can be translated into a condition of $\alpha = D/F$: $\alpha > 30 l_0/F$. If the aperture diameter is about four times l_0 (i.e. too small) the overestimation of C_{n^2} is at its maximum and is of the order of 35 %.

2.7.2 The effect of the outer scale

The shape of the spectral density function at low wave numbers depends on the flow geometry and the mechanisms of turbulence production. Therefore this region of the spectrum does not have a universal shape. One approximation that is often used is (a variant of) the Von Karman spectrum (Strohbehn, 1968):

$$\Phi_{nn}(\kappa) = \alpha\left(1 + \kappa^2\mathcal{L}_0^2\right)^{-11/6}\exp(\kappa^2/\kappa_m^2)\,, \tag{2.39}$$

where $\alpha = \sigma_n^2\mathcal{L}_0^3\pi^{-3/2}\Gamma(\frac{11}{6})/\Gamma(\frac{1}{3})$ and it has been assumed that $\kappa_m\mathcal{L}_0 \gg 1$. The correction for high wave numbers from the Tatarski-spectrum has been included as well. In order for the values of the model

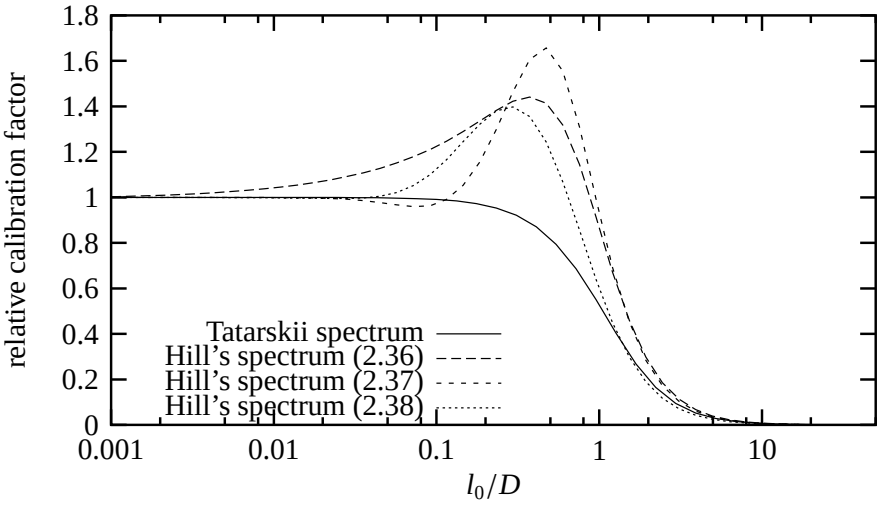

Figure 2.9: Dependence of the calibration of the LAS on the micro scale (using the Tatarski spectrum (2.35) and Hill's spectra (2.36), (2.37) and (2.38)). For this plot $\alpha = 5$ and $F = 0.0305m$. The calibration factor has been normalized such that the calibration for infinitely small l_0 equals 1. Note that Hill's spectrum from equation (2.38) fits the experimental spectra best.

spectrum in (2.39) to be equal to those of the Tatarski spectrum (2.35), one needs to assume a relationship between the variance of n and the structure function parameter C_{n^2} (Strohbehn, 1968):

$$C_{n^2} \approx 1.9\sigma_n^2 \mathcal{L}_0^{-2/3} . \tag{2.40}$$

In figure 2.10 one can see that for the outer scale $\mathcal{L}_0$ to have negligible influence on the calibration of the LAS, the beam diameter should at least be ten times the macro length scale. This is in line with the claim of Hill and Ochs (1978) that the outer scale should be *much* larger than three times the aperture diameter. For surface layer turbulence the outer scale could be estimated as the distance to the surface. So given a beam diameter of 0.15 *m*, the minimum height of the beam above the ground should be 1.5 *m*.

2.8 Summary of the assumptions

In the derivations in the previous sections a number of assumptions has been made. Some of the assumptions made in the derivation of the log amplitude variance for the infinitely small transmitter and receiver (section 2.5) are overridden by less restrictive assumptions when the scattering theory is applied to the LAS. Here only the restrictions applicable to the LAS will be listed.

The assumptions needed to arrive at equation (2.34) are:

- Variations in the refractive index must much less than 1: $n = 1 + n_1$ with $n_1 \ll 1$ (on page 8).
- The inner scale l_0 must be much larger than the wave length of the radiation used: $l_0 \gg \lambda$ (2.5 on page 8), but Lee and Harp (1969) have shown that this restriction may be irrelevant.
- The turbulent field is *locally* isotropic (on page 9).
- One has to assume a Kolmogorov type spectrum ($\Phi_{nn}(\kappa) \sim \kappa^{-11/3}$) for the wave number of the inhomogeneities that result in intensity fluctuations at the detector. This implies that these relevant wave numbers must correspond to sizes between the outer scale $\mathcal{L}_0$ and the inner scale l_0 (see section 2.5). For infinitely small transmitters and receivers the most active inhomogeneities (near the centre of the path) are of the order of the diameter of the first Fresnel zone ($\sqrt{\lambda L}$, see on page 9). For the LAS the size of the relevant inhomogeneities is of the order of the aperture diameter (see page 2.6.4 on page 17). Thus in that case the aperture diameter must be in between the inner scale and the outer scale. This implies that D should be 30 to 50 times the inner scale (inner scale, see 2.7.1) and the outer scale should be more than ten times larger than the aperture diameter (see section 2.7.2).

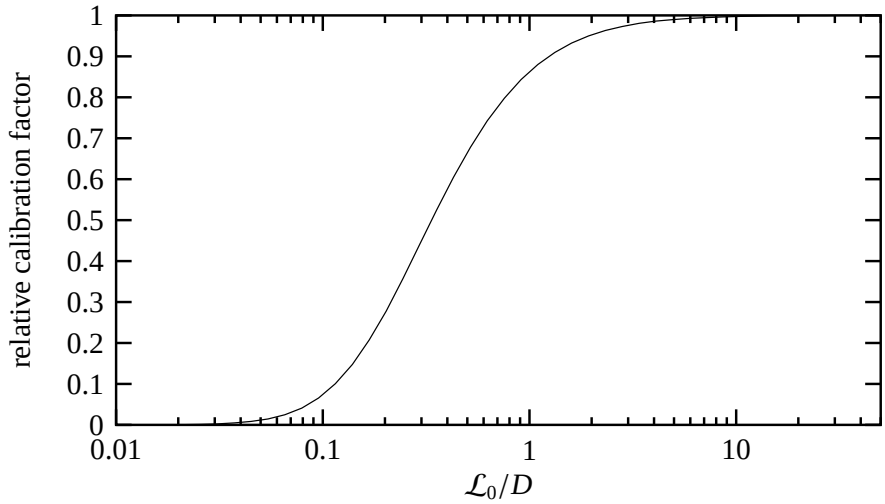

Figure 2.10: Dependence of the calibration of the LAS on the outer scale using the Strohbehn spectrum (2.39). For this plot $\alpha = 5$ and $F = 0.0305m$. The calibration factor has been normalized such that the calibration for infinitely large $\mathcal{L}_0$ equals 1.

- The aperture diameter must be sufficiently large to prevent saturation effects: $\alpha \gg 1.6\sqrt{\sigma^2_{\chi,0}}$ (section 2.6.2 on page 15).
- The diameter of the aperture of the LAS must be much larger than the diameter of the first Fresnel zone (at least twice): $D \gg \sqrt{\lambda L}$ (see section 2.6.2 on page 16)

3 C_{T^2} derived from C_{n^2}

In order to relate the structure function parameter of the refractive index, C_{nn} to the the structure function parameter of certain air properties (notably temperature and water vapour content), it is necessary to first explore the dependence of the refractive index on the given properties of the air. Then expressions are sought for the fluctuations of n as a function of the fluctuations of the state variables. In turn these expressions are used to relate the various structure function parameters. Here, the focus is on scintillometers operating in the near-infrared part of the spectrum. But scintillometers operating at other wavelengths have been used as well, most notably radio-wave scintillometers (Kohsiek and Herben, 1983; Meijninger *et al.*, 2002*a*). At radio-wave wavelengths, the refractive index is mainly determined by water vapour content, making radio-wave scintillometers appropriate for the direct estimation of evaporation.

3.1 Dependence of the refractive index on wavelength and air properties

The refractive index of a gas depends on the composition of the gas, and it's state variables: pressure and temperature. Given the fact that in air under atmospheric conditions water vapour is by far the most variable constituent of air, the composition of air can be described in terms of dry air and water vapour. Therefore in general the refractive index can be written as:

$$n = n(\lambda, p, T, q)\,, \tag{3.1}$$

where p is the atmospheric pressure (in Pa), T is the absolute temperature (in K) and q is the specific humidity (in $kgkg^{-1}$). Thus for a given wavelength the refractive index depends on p, T and q (or equivalently the water vapour pressure e). The functional dependence of n on the state variables can be derived from the Lorenz-Lorentz law (see e.g. Jenkins and White (1976) and McCartney (1976)) according to which

$$\frac{n^2-1}{n^2+2} = (n-1)\,\frac{n+1}{n^2+2} \sim \rho\,. \tag{3.2}$$

When n is close to unity, the factor $\frac{n+1}{n^2+2}$ is nearly constant. When furthermore a reference condition is defined (indicated by a subscript 0, e.g. n_0) the Lorenz-Lorentz law can be rewritten as:

$$n - 1 = \frac{\rho}{\rho_0}\,(n_0 - 1) \tag{3.3}$$

Feynman *et al.* (1989) gives a theoretical relationship for n which state that for a substance with n close to 1:

$$n - 1 \sim \sum_k \frac{N_k}{\omega_k^2 - \omega^2}\,, \tag{3.4}$$

where ω_k is the resonant frequency of an electron in an atom, N_k is the number of electrons with a given resonant frequency and the summation is over all types of electrons in the substance (see Feynman *et al.* (1989) for a more precise explanation) [1].

[1] From the theoretical model for n it appears that it is the number density of electrons with a given resonant frequency that determines the refractive index rather than the mass density of each species. But this difference is obfuscated in the various empirical relationships for the refractive index.

Absorbing the reference variables in (3.3) in a constant A, using the ideal gas law and splitting the mixture in the k constituting species this can be rewritten as [2]:

$$n - 1 = \frac{1}{RT} \sum_k A_k M_k p_k \,, \tag{3.5}$$

where R is the universal gas constant, M_k is the molar mass of species k and p_k is the partial pressure of species k.

The wavelength dependence of the refractive index is then restricted to the wavelength dependence of the constant A (and thus n_0). A number of empirical expressions for the refractive index of air as a function of wavelength (and pressure, temperature and humidity content) are known which have the general form:

$$n - 1 = m_1(\lambda)\frac{p}{T} + m_2(\lambda)\frac{e}{T} \,, \tag{3.6}$$

where p is the total air pressure (the partial pressure for dry air is $p - e$; the term containing e that would appear in (3.5) for the species 'dry air' has been absorbed in the second term). In the sequel, m_1 and m_2 will have units of KPa^{-1}.

The relationships from Barrell and Sears (as can be found for instance in List (1971) or Friehe *et al.* (1975)) for the wavelength range corresponding to visible light, $283K < T < 303K$ and $960hPa < p < 1067hPa$ are:

$$m_1(\lambda) = \left(0.774701 \cdot 10^{-6} + 4.38728 \cdot 10^{-9}\lambda^{-2} + 0.36738 \cdot 10^{-9}\lambda^{-4}\right) f(p,T) \tag{3.7a}$$

$$m_2(\lambda) = -0.12785 \cdot 10^{-6}(1 - 0.0109\lambda^{-2}) \tag{3.7b}$$

with $f(p,T) = 1 + (40.03 - 0.118T) \cdot 10^{-9}p$. The term with λ^{-4} in the numerator is not in line with the theoretical model for n (see (3.4) and recall that $\lambda \sim \omega^{-1}$).

Owens (1967) (cited in Andreas (1988) gives, for $0.36\mu m < \lambda < 3\mu m$:

$$m_1(\lambda) = 0.237134 \cdot 10^{-6} + \frac{68.39397 \cdot 10^{-6}}{130 - \lambda^{-2}} + \frac{0.45473 \cdot 10^{-6}}{38.9 - \lambda^{-2}} \tag{3.8a}$$

$$m_2(\lambda) = -m_1(\lambda) + 0.648731 \cdot 10^{-6} + 0.0058058 \cdot 10^{-6}\lambda^{-2} - 0.071150 \cdot 10^{-9}\lambda^{-4} + 0.008851 \cdot 10^{-9}\lambda^{-6} \tag{3.8b}$$

In Hill *et al.* (1980) the following relationship can be found (they cite Goody (1965)):

$$m_1(\lambda) = \left(0.18282 \cdot 10^{-6} + \frac{83.833 \cdot 10^{-6}}{146 - \lambda^{-2}} + \frac{0.7258 \cdot 10^{-6}}{41 - \lambda^{-2}}\right) f(p,T) \tag{3.9a}$$

$$m_2(\lambda) = -0.12766 \cdot 10^{-6}(1 - 0.0109\lambda^{-2}) \tag{3.9b}$$

with $f(p,T) = 1 + (40.03 - 0.118T) \cdot 10^{-9}p$. The relationships given in (3.8) and (3.9) are in line with the theoretical relationships (3.4). Equation (3.9) seems to be a mixture of (3.7) and (3.8).

In figure 3.1 the different expressions for m_1 and m_2 are compared. It appears that for the wavelength used in the LAS of Wageningen University (i.e. $0.94\ \mu m$) the values for m_1 and m_2 are equal within less than 2 %.

Given the observation that the resonant frequencies of electrons occurring in air correspond to ultraviolet light (i.e. frequencies much higher than that of visible light), in (3.4) ω^2 is negligible with respect to ω_k^2. Thus the wavelength dependence of the refractive index for visible light is only very weak.

3.2 Fluctuations in the refractive index due to fluctuations in state variables

In the previous section an experession was given for n as a function of the state variables p and T, composition e and a wavelength dependence through m_1 and m_2: equation (3.6).

[2] The factor $A = \frac{n_0 - 1}{\rho_0}$ is different per species. From the considerations in Feynman *et al.* (1989) it can be seen that $n - 1$ of a mixture is the sum of contributions of te species. Furthermore, it should be noted that the effect of absorption on the refractive index, i.e. anomalous refraction, is not dealt with here (see e.g. Hill *et al.* (1980)).

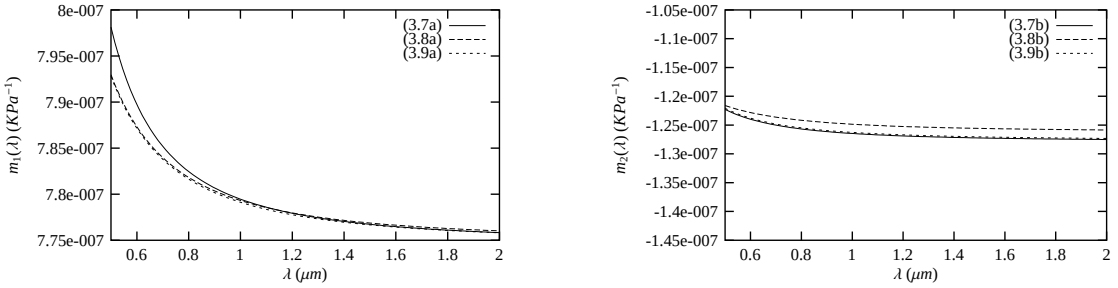

(a) (b)

Figure 3.1: The wavelength dependence of the different expressions for $m_1(\lambda)$ and $m_2(\lambda)$ (equations (3.7), (3.8) and (3.9)) is shown for a range of wavelength in the visible and near infrared range (the wavelength used in the LAS of Wageningen University is 0.94 μm. The pressure and temperature dependence in (3.7a) and (3.9a) has been neglected.

Since we are dealing with a turbulent medium it is customary to decompose the variables into an *ensemble mean* and a fluctuating part:

$$n = \overline{n} + n' \tag{3.10a}$$
$$p = \overline{p} + p' \tag{3.10b}$$
$$e = \overline{e} + e' \tag{3.10c}$$
$$T = \overline{T} + T' \tag{3.10d}$$

To first order in the fluctuations, the fluctuation in n can be written in terms of the fluctuations and mean values of p, e and T, using the fractional change in n as a function of these variables:

$$n' = \frac{\partial n}{\partial p}p' + \frac{\partial n}{\partial e}e' + \frac{\partial n}{\partial T}T' \tag{3.11}$$

where the derivatives are evaluated at the reference values of p, e and T, viz. $\overline{p}$, $\overline{e}$ and $\overline{T}$. With (3.6) and omitting those terms with derivatives that are zero in (3.11), the latter can be written as:

$$n' = m_1\frac{\overline{p}}{T}\frac{p'}{\overline{p}} - m_1\frac{\overline{p}}{T}\frac{T'}{\overline{T}} + m_2\frac{\overline{e}}{T}\frac{e'}{\overline{e}} - m_2\frac{\overline{e}}{T}\frac{T'}{\overline{T}}\,, \tag{3.12}$$

or:

$$n' = A_p\frac{p'}{\overline{p}} + A_e\frac{e'}{\overline{e}} + A_T\frac{T'}{\overline{T}}\,, \tag{3.13}$$

where $A_x = \overline{x}\frac{\partial n}{\partial x}$ (x is either p, e or T):

$$A_p = \overline{p}\frac{\partial n}{\partial p} = m_1\frac{\overline{p}}{\overline{T}} \tag{3.14a}$$
$$A_e = \overline{e}\frac{\partial n}{\partial e} = m_2\frac{\overline{e}}{\overline{T}} \tag{3.14b}$$
$$A_T = \overline{T}\frac{\partial n}{\partial T} = -m_1\frac{\overline{p}}{\overline{T}} - m_2\frac{\overline{e}}{\overline{T}} \tag{3.14c}$$

Thus the coefficients A_p, A_e and A_T do depend on the wavelength of the light under consideration –through m_1 and m_2 as well as on the state and composition of the air.

Up to this point the partial pressure of water vapour has been used to specify the concentration of water vapour. But alternative parameters are used as well, in particular the water vapour density, ρ_v and the specific humidity, q.

With the use of the gas law it can easily be deduced that the influence of water vapour on the refractive index is $m_2 R_v \rho_v$, which leads to

$$A_{\rho_v} = m_2 R_v \overline{\rho}_v \,, \tag{3.15}$$

where R_v is the specific gas constant for water vapour. For specific humidity the procedure is less straightforward. The second term in (3.6) (we will call it n_w although strictly speaking the first term also carries some water vapour influence) can be written as:

$$n_w = m_2 R_v \rho q = m_2 \frac{R_v}{R} \frac{p}{T} q \,. \tag{3.16}$$

Now n_w not only depends on the amount of water vapour and the temperature, but on the pressure as well. The water vapour dependency is present in two places: directly in q and indirectly in R. The fractional change of n_w as a function of the different variables becomes now:

$$\begin{aligned} {n_w}' &= \frac{\partial n_w}{\partial p} p' + \frac{\partial n_w}{\partial q} q' + \frac{\partial n_w}{\partial T} T' \\ &= \overline{n}_w \frac{p'}{\overline{p}} + \overline{n}_w \frac{q'}{\overline{q}} - \frac{\overline{n}_w}{R} \frac{\partial R}{\partial q} q' - \overline{n}_w \frac{T'}{\overline{T}} \,, \end{aligned} \tag{3.17}$$

which leads to the following expression for A_q:

$$A_q = \overline{q} m_2 \frac{R_v}{R} \frac{\overline{p}}{\overline{T}} \left(1 - \frac{1}{R} \frac{\partial R}{\partial q} \right) . \tag{3.18}$$

The second term between parentheses can be evaluated as follows:

$$\begin{aligned} \frac{1}{R} \frac{\partial R}{\partial q} &= M \frac{\partial \frac{1}{M}}{\partial q} \\ &= \left(\frac{\overline{q}}{M_v} + \frac{1-\overline{q}}{M_d} \right)^{-1} \left(\frac{1}{M_v} - \frac{1}{M_d} \right) \\ &= \left(\overline{q} \frac{M_d}{M_v} + (1-\overline{q}) \right)^{-1} \left(\frac{M_d}{M_v} - 1 \right) \end{aligned} \tag{3.19}$$

where M, M_v and M_d are the molar masses of moist air, water vapour and dry air respectively. Here use has been made of the fact that $\frac{1}{M} = \frac{q}{M_v} + \frac{1-q}{M_d}$. The complete expression for A_q becomes:

$$A_q = \overline{q} m_2 \frac{M_d}{M_v} \frac{\overline{p}}{\overline{T}} \left(\overline{q} \frac{M_d}{M_v} + (1-\overline{q}) \right)^{-2} \left(\frac{M_d}{M_v} - 1 \right) \tag{3.20}$$

If the moisture content dependence of M is to be neglected, the latter becomes equal to:

$$A_q \approx \overline{q} m_2 \frac{M_d}{M_v} \frac{\overline{p}}{\overline{T}} \left(\frac{M_d}{M_v} - 1 \right) \tag{3.21}$$

The error in A_q due to negligence of the water vapour dependence of R ranges from nil when $\overline{q} = 0$ to 3.5% when $\overline{q} = 0.03 kg kg^{-1}$ (the dependence of the error on q is nearly linear).

The next step is to evaluate the relative importance of the successive terms in (3.13). To this end a table has been compiled containing representative values for $\overline{x}$, x' and A_x (for x is p, e and T) under atmospheric conditions (see table 3.1).

From this table a number of conclusions can be drawn. At the given wavelength, the effect of temperature fluctuations on the refractive index is by far the most important. It is two orders of magnitude larger than the effect of humidity fluctuations. In turn, the effect of pressure fluctuations is more than two orders of magnitude smaller than the humidity effect. This leads to the customary assumption that the effect of pressure fluctuations on the refractive index can be safely ignored, except for rare cases where both temperature and humidity fluctuations are very small. The effect of temperature fluctuations and humidity fluctuations on the structure parameter of the refractive index will be dealt with in the next section.

		turbulent variable x				
variable	unit	mean	turbulent fluctuation	relative fluctuation	A_x	$A_x \frac{x'}{\overline{x}}$
p	Pa	10^5	0.01	10^{-7}	$0.26 \cdot 10^{-3}$	$26 \cdot 10^{-12}$
q	$kgkg^{-1}$	10^{-2}	10^{-4}	10^{-2}	$-0.67 \cdot 10^{-6}$	$-6.7 \cdot 10^{-9}$
T	K	300	1	$3 \cdot 10^{-3}$	$-0.26 \cdot 10^{-3}$	$-0.78 \cdot 10^{-6}$

Table 3.1: Representative value for the mean value and fluctuation of p, e and T, as well as the corresponding value for A. For the evaluation of m_1 and m_2 the relationships in (3.9) have been used with a wavelength of 940 nm, which corresponds to the wavelength of the LED used in the LAS of the Meteorology and Air Quality group of Wageningen University. This results in the following values: $m_1 = 0.780 \cdot 10^{-6} KPa^{-1}$ (at the given precision inclusion of the correction factor $f(p,T)$ with $T = 288K$ and $p = 10^5 Pa$ does not influence the result) and $m_2 = -0.126 \cdot 10^{-6} KPa^{-1}$. The relative fluctuation $x'/\overline{x}$ is given as an estimate for $\sqrt{C_{xx}}/\overline{x}$. The value for p' has been estimated from the assumption $p' \sim \rho u'^2$ with $u' \approx 0.1 ms^{-1}$.

3.3 The relationship between C_{n^2} and C_{T^2}, C_{Tq} and C_{q^2}

The analysis presented in the section is part of Moene (2003)

In order to find the relationship between the structure function parameter of the refractive index on one hand, and the structure function parameters of state variables on the other hand, we revert to the definition of the structure function for a homogeneous flow (see (2.4)). For separations r within the inertial subrange this becomes:

$$\begin{aligned} D_{nn}(r) &= 2\left(B_{nn}(0) - B_{nn}(r)\right) \\ &= 2\left(\overline{n'n'} - \overline{n'(x)n'(x+r)}\right) \\ &= C_{n^2} r^{2/3} \end{aligned} \tag{3.22}$$

Inserting the approximation for $\overline{n}$ as a function of p, e and T (3.6) into (3.22) we obtain:

$$\begin{aligned} \frac{1}{2} C_{n^2} r^{2/3} = &\overline{\left(A_p \frac{p'}{\overline{p}} + A_q \frac{q'}{\overline{q}} + A_T \frac{T'}{\overline{T}}\right)^2} - \\ &\overline{\left(A_p \frac{p'(x)}{\overline{p}} + A_q \frac{q'(x)}{\overline{q}} + A_T \frac{T'(x)}{\overline{T}}\right)\left(A_p \frac{p'(x+r)}{\overline{p}} + A_q \frac{q'(x+r)}{\overline{q}} + A_T \frac{T'(x+r)}{\overline{T}}\right)} \end{aligned} \tag{3.23}$$

Evaluation of all products finally leads to:

$$C_{n^2} = \frac{A_p A_p}{\overline{p}\overline{p}} C_{pp} + \frac{A_q A_q}{\overline{q}\overline{q}} C_{q^2} + \frac{A_T A_T}{\overline{T}\overline{T}} C_{T^2} + 2\frac{A_p A_q}{\overline{p}\overline{q}} C_{pq} + 2\frac{A_p A_T}{\overline{p}\overline{T}} C_{pT} + 2\frac{A_q A_T}{\overline{q}\overline{T}} C_{qT} \tag{3.24}$$

As was shown in the previous section, the effect of pressure fluctuations can be ignored in most cases. Therefore the terms in (3.24) containing C_{pp}, C_{pT} and C_{pq} will be ignored from this point onwards. Thus only the terms containing either T or q are retained.

Usually, little information is available on the cross-structure parameter C_{Tq} and on C_{qq}. Therefore it is customary to eliminate C_{Tq} and C_{qq} with the use of some other information on the relationship between T and q fluctuations, viz. the Bowen ratio β and the correlation coefficient between T and q. Wesely and Alcaraz (1973) just pose a relationship –without derivation– between C_{T^2} and C_{n^2} involving the Bowen ratio. Wesely (1976*a*) gives a derivation for the relationship between C_{T^2} and C_{n^2} and uses the relationship $\sqrt{C_{T^2}/C_{q^2}} = \overline{w'T'}/\overline{w'q'}$ to introduce the Bowen ratio. Kohsiek (1982) shows that indeed a close relationship between $\sqrt{C_{T^2}/C_{q^2}}$ and $\overline{w'T'}/\overline{w'q'}$ exists (albeit with considerable scatter, which is obscured by the use of a double log-plot: figure 14 in Kohsiek (1982)). Another important point to note is that in the present context the correlation between T and q is needed at the scales that are seen by the scintillometer, i.e. scales that are of the order of the beam diameter and that should be located in the inertial subrange (see section 2.6.4). There is evidence that the correlation coefficient in the inertial subrange is rather constant with frequency and nearly equal to the correlation coefficient integrated over the entire spectrum, i.e. $\overline{T'q'}/(\sigma_T \sigma_q)$ (see Kohsiek (1984)).

In the sequel a slightly different and more clear derivation will be given for the elimination of C_{Tq} and C_{q^2} from (3.24).

First the expression for the structure function parameter in the inertial subrange will be rewritten. To that end the cross-correlation function R_{Tq} is estimated from the auto-correlation functions of T and q as well as the correlation coefficient $R_{Tq}(0)$:

$$R_{Tq}(r) \approx R_{Tq}(0)\sqrt{R_{TT}(r)R_{qq}(r)}\,. \tag{3.25}$$

This approximation will be valid as long as the spatial structures of T and q are similar (in terms of micro scale and macro scale). In fact, the correlation coefficient between T and q in the inertial subrange is assumed to be constant and equal to the correlation coefficient integrated over the entire spectrum. This assumption is supported to some extent by the results of Wyngaard *et al.* (1978) who show that the Tq-cospectrum has an inertial subrange behaviour similar to that of the T-spectrum and q-spectrum. Equation (3.25) also corresponds to the relationship $C_{Tq} = R^K_{Tq}\sqrt{C_{T^2}C_{q^2}}$ (where R^K_{TQ} is the inertial subrange correlation coefficient between T and q) given by Kohsiek (1982), which was derived based on assumptions about the similarity relationships for C_{T^2}, C_{Tq} and C_{q^2}.

Given the approximation in (3.25), the expressions for the structure functions parameters C_{Tq} and C_{q^2} (no approximation involved) become:

$$\frac{1}{2}C_{Tq}r^{2/3} \approx R_{Tq}(0)\left(1-\sqrt{R_{TT}(r)R_{qq}(r)}\right)\sigma_T\sigma_q \tag{3.26a}$$

$$\frac{1}{2}C_{q^2}r^{2/3} = \left(1-R_{qq}(r)\right)\sigma_q^2 \tag{3.26b}$$

where σ_T is the standard deviation of T and $R_{Tq}(r)$ is the correlation coefficient between T and q on locations separated by a distance r. With the aid of these expressions C_{Tq} and C_{q^2} can be expressed in terms of C_{T^2}, the ratio σ_q/σ_T and the correlation coefficient R_{Tq}:

$$C_{Tq} \approx C_{T^2}R_{Tq}(0)\frac{1-\sqrt{R_{TT}(r)R_{qq}(r)}}{1-R_{TT}(r)}\frac{\sigma_q}{\sigma_T} \tag{3.27a}$$

$$C_{q^2} = C_{T^2}\frac{1-R_{qq}(r)}{1-R_{TT}(r)}\left(\frac{\sigma_q}{\sigma_T}\right)^2\,. \tag{3.27b}$$

Provided that the spatial structures of T and q in the inertial subrange are identical (i.e. $R_{qq}(r)$ equals $R_{TT}(r)$)[3], (3.27b) can be simplified to:

$$C_{Tq} \approx C_{T^2}R_{Tq}(0)\frac{\sigma_q}{\sigma_T} \tag{3.28a}$$

$$C_{q^2} \approx C_{T^2}\left(\frac{\sigma_q}{\sigma_T}\right)^2 \tag{3.28b}$$

Now (3.24) can be simplified and expressed as a relationship between C_{n^2} and C_{T^2}:

$$C_{n^2} = \frac{A_TA_T}{\overline{TT}}C_{T^2}\left(1+2\frac{A_q}{\overline{q}}\frac{\overline{T}}{A_T}R_{Tq}(0)\frac{\sigma_q}{\sigma_T}+\frac{A_qA_q}{\overline{qq}}\frac{\overline{TT}}{A_TA_T}\left(\frac{\sigma_q}{\sigma_T}\right)^2\right) \tag{3.29}$$

Thus in principle one could derive C_{T^2} from C_{n^2} with only mean values and variances of T and q as well as the correlation coefficient $R_{Tq}(0)$ as additional data. In order to compare this result with the commonly used expression which contains the Bowen ratio, the ratio σ_q/σ_T needs to be linked to the Bowen ratio. The latter is given by:

$$\beta = \frac{H}{L_vE} = \frac{c_p}{L_v}\frac{\overline{w'T'}}{\overline{w'q'}}\,, \tag{3.30}$$

[3] Note that this does not necessarily imply $R_{Tq}(0) = 1$.

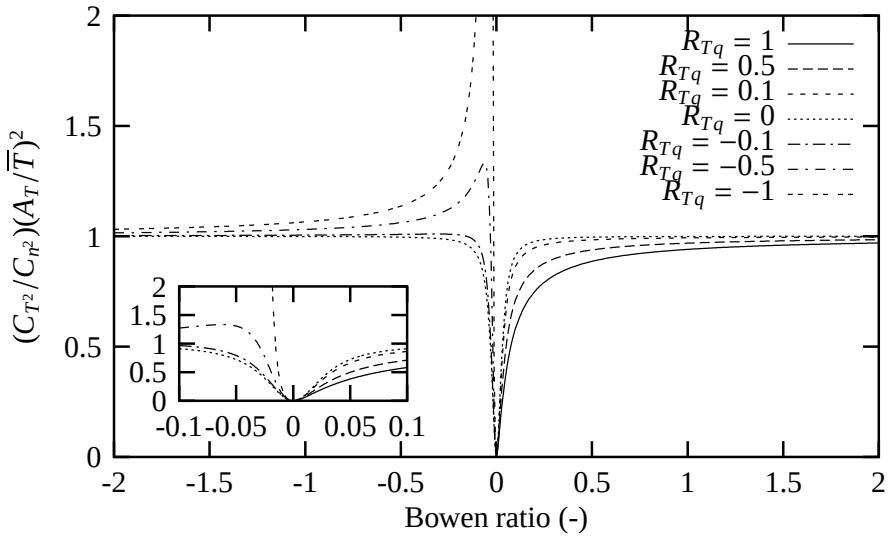

Figure 3.2: Correction factor in (3.32), i.e. $\frac{C_{n^2}}{C_{T^2}} \frac{\overline{TT}}{A_T A_T}$. The inset shows the details around $\beta = 0$.

where H is the sensible heat flux, E is the evapotranspiration, L_v is the latent heat of vaporation, c_p is the specific heat at constant pressure and w is the vertical velocity. (3.30) can be rewritten, without any assumptions as:

$$\beta = \frac{c_p}{L_v} \frac{\sigma_T}{\sigma_q} \frac{R_{wq}}{R_{wT}} \,. \tag{3.31}$$

Thus if the assumption that R_{wq} equals R_{wT} is made, the Bowen ratio can be linked directly to the ratio of the standard deviations of temperature and specific humidity. It is very important to note that $R_{wq} = R_{wT}$ does *not* necessarily imply $R_{Tq} = 1$[4]. Under the assumption that $R_{wq} = R_{wT}$ expression (3.31) will always give a positive Bowen ratio, which is consistent with the assumption. However, if the fluxes of water vapour and heat would go in opposite directions, $R_{wq} = -R_{wT}$. Therefore the absolute value of β needs to be used when R_{wq}/R_{wT} is set to unity.

From this point it is possible to express C_{n^2} in terms of C_{T^2} and the Bowen ratio:

$$C_{n^2} = \frac{A_T A_T}{\overline{TT}} C_{T^2} \left(1 + 2 \frac{A_q}{\overline{q}} \frac{\overline{T}}{A_T} R_{Tq}(0) \frac{c_p}{L_v} |\beta|^{-1} + \frac{A_q A_q}{\overline{qq}} \frac{\overline{TT}}{A_T A_T} \left(\frac{c_p}{L_v} \right)^2 |\beta|^{-2} \right) \tag{3.32}$$

Figure 3.2 shows the magnitude of the correction factor as a function of the Bowen ratio and for various values for R_{Tq}. When the additional assumption is made that $|R_{Tq}| = 1$, and when the information about the sign of R_{Tq} is taken from the sign of β (i.e. $|\beta|$ is replaced by β), (3.32) can be written as:

$$C_{n^2} = \frac{A_T A_T}{\overline{TT}} C_{T^2} \left(1 + \frac{A_q}{\overline{q}} \frac{\overline{T}}{A_T} \frac{c_p}{L_v} \beta^{-1} \right)^2 \tag{3.33}$$

The factor in front of β^{-1} is, for the atmospheric conditions used in table 3.1 equal to 0.031, which is consistent with the value quoted by Wesely (1976*a*). But it is important to keep in mind that this factor does depend on the atmospheric conditions.

In Moene (2003) the various assumptions used in the derivation above are confronted with experimental data. Furthermore, the effect of those approximations on the various estimates of C_{T^2} from C_{n^2} (equations (3.29), (3.32), and (3.33)) are given.

[4] Of course, the other way around the relationship is clear: if $R_{Tq} = 1$, then $R_{wq} = R_{wT}$ (see de Bruin *et al.*, 1993; Hill, 1989).

3.4 Summary of the assumptions

The purpose of the present section was to find the relationship between the structure function parameter of the refractive index, C_{n^2} and the structure function parameter of temperature, C_{T^2}. Along the way a number of assumptions has been made, which will be summarized here.

- In order simplify the Lorenz-Lorentz law it was assumed that the refractive index is close to unity, which is a fair assumption for air.
- The assumption that $n - 1 \ll 1$ has also been used in the various empirical relationships that link $n - 1$ for air to the wavelength of the light under consideration and the variables that describe the state of the air. For some of these empirical relationships it is unclear for which range of atmospheric conditions they hold.
- Dependence of $n - 1$ on the composition of air is neglected, except for the dependence on water vapour content.
- The dependence of fluctuations of n on fluctuations in the state variables and the water vapour content is described using the fractional change of $\frac{\partial n}{\partial x}$ where x is one of the variables. This description is valid to first order in the fluctuations.
- If the water vapour dependence of M is neglected in the computation of A_q (see 3.2 on page 26), this can give an error in A_q between 0 and 3.5 %, when q ranges from 0 to $0.03 kg \cdot kg^{-1}$.
- The relative fluctuations (for variable x: $x'/\overline{x}$) in the pressure are assumed to be about five orders smaller than the relative fluctuations in temperature and specific humidity (see table 3.1).
- In the elimination of C_{Tq} and C_{q^2} from C_{n^2} it has been assumed that the spatial structure of the temperature and humidity fields are identical in the inertial subrange (i.e. $R_{TT}(r) = R_{qq}(r)$).
- In order to express C_{n^2} in terms of C_{T^2}, the Bowen ratio and R_{Tq} it has been assumed that $|R_{wT}| = |R_{wq}|$, but it was *not* necessary to assume $R_{Tq} = 1$.
- To eliminate the dependence of C_{n^2} on R_{Tq} some assumption with respect to R_{Tq} needs to be made (for instance that $R_{Tq} = 1$).

4 Sensible heat flux H derived from C_{T^2}

The final step in the application of the scintillometer in the determination of the sensible heat flux is the link between H and C_{T^2}. This link is derived from Monin-Obukhov similarity relationships for C_{T^2} (section 4.1). Since in the similarity relationships not only H and C_{T^2} occur, additional data are needed to obtain H from C_{T^2} (section 4.2). Finally, section 4.3 gives an overview of all data that are needed to derive H from the actual output of the scintillometer, i.e. the log intensity variance, $\sigma^2_{ln(I)}$.

4.1 Similarity relationships for C_{T^2}

In order to derive the surface sensible heat flux from C_{T^2} a relationship between the two is needed. This relationship can be found in the surface layer similarity relationship for C_{T^2}. Using Monin-Obukhov similarity (MOS) this can generally be stated as:

$$\frac{C_{T^2}(z-d)^{2/3}}{\theta_*^2} = \Phi_{TT}\left(\frac{z-d}{L_{MO}}\right), \tag{4.1}$$

with:

$$\theta_* = \frac{H}{u_* \rho c_p} \tag{4.2}$$

$$u_* = \sqrt{\frac{\tau_0}{\rho}}$$

$$L_{MO} = \frac{g}{\overline{T}} \frac{\theta_*}{u_*^2} \tag{4.3}$$

where z is the height above the ground and d is the zero plane displacement height, θ_* is the MOS temperature scale, u_* is the friction velocity, τ_0 is the surface shear stress, L_{MO} is the Obukhov length, g is the gravitational acceleration and $\overline{T}$ is the mean ambient temperature (in K !). In fact, (4.1) describes the stability dependence of C_{T^2}. Several expressions for Φ_{TT} can be found in literature. As with most MOS similarity relationships, the relationships are split into separate expressions for for stable ($\frac{z-d}{L_{MO}} > 0$) and unstable ($\frac{z-d}{L_{MO}} < 0$) conditions. Table 4.1 and 4.2 give an overview of the different relationships for unstable and stable conditions, respectively. Graphs of the respective expressions are given in figures 4.1 and 4.2.

In figure 4.1 it can be seen that the various expressions for $f\left(\frac{z-d}{L_{MO}}\right)$ for unstable conditions correspond to within roughly 20%, except for the expressions by Hill *et al.* (1992) and Thiermann and Grassl (1992). For stable conditions (figure 4.2) the expressions correspond to within about 25%, except for that of de Bruin *et al.* (1993). Recently, Hoedjes *et al.* (2002) studied the similarity relationships for the structure parameters under stable conditions during daytime (conditions of strong evaporation).

4.2 Combination of similarity relationships for C_{T^2} with other data to obtain H

In order to derive a sensible heat flux from (4.1), one also needs u_*. This can either be measured directly, or be obtained —using similarity relationships— from mean wind speed measurements (either at two heights,

formula	coefficients	reference
$c_{TT1}\left(1 - c_{TT2}\frac{z-d}{L_{MO}}\right)^{-2/3}$	$c_{TT1} = 4.9$, $c_{TT2} = 7$	Wyngaard *et al.* (1971)
$c_{TT1}\left(1 - c_{TT2}\frac{z-d}{L_{MO}}\right)^{-2/3}$	$c_{TT1} = 4.9$, $c_{TT2} = 7$	Wyngaard (1973)
$c_{TT1}\left(1 - c_{TT2}\frac{z-d}{L_{MO}}\right)^{-2/3}$	$c_{TT1} = 4.9$, $c_{TT2} = 6.1$	Andreas (1988) [a]
$\left(1 + c_{TT1}(\frac{z-d}{L_{MO}} + c_{TT3}) + c_{TT2}(\frac{z-d}{L_{MO}} + c_{TT3})^{10}\right)^{-2}$	$c_{TT1} = 0.45$, $c_{TT2} = 0.01$, $c_{TT3} = 1.5$	Wesely (1976*b*)
$c_{TT1}\left(1 - c_{TT2}\frac{z-d}{L_{MO}}\right)^{-2/3}$	$c_{TT1} = 4.9$, $c_{TT2} = 9$	de Bruin *et al.* (1993)
$c_{TT1}\left(1 + c_{TT2}\lvert\frac{z-d}{L_{MO}}\rvert\right)^{-2/3}$	$c_{TT1} = 8.1$, $c_{TT2} = 15$	Hill *et al.* (1992) [b]
$4k^{-2/3}\beta_1\left(1 - c_{TT2}\frac{z-d}{L_{MO}} + c_{TT3}\left(\frac{z-d}{L_{MO}}\right)^2\right)^{-1/3}$	$\beta_1 = 0.86$, $c_{TT2} = 7$, $c_{TT3} = 75$	Thiermann and Grassl (1992) [c]

[a] adjustment of Wyngaard (1973) reflecting the change of Von Karman constant from 0.35 to 0.4
[b] adjustment of Wyngaard *et al.* (1971) to better fit near-neutral data
[c] β_1 is the Obukhov-Corrsin constant, k is the Von Karman constant

Table 4.1: Overview of similarity relationships $\Phi_{TT}\left(\frac{z-d}{L_{MO}}\right) = C_{T^2}\theta_*^{-2}(z-d)^{2/3}$ for unstable conditions.

formula	coefficients	reference
$c_{sTT1}\left(1 + c_{sTT2}\frac{z-d}{L_{MO}}\right)$	$c_{sTT1} = 4.9$, $c_{sTT2} = 2.75$	Wyngaard *et al.* (1971)
$c_{sTT1}\left(1 + c_{sTT2}\left(\frac{z-d}{L_{MO}}\right)^{2/3}\right)$	$c_{sTT1} = 4.9$, $c_{sTT2} = 2.4$	Wyngaard (1973)
$c_{sTT1}\left(1 + c_{sTT2}\left(\frac{z-d}{L_{MO}}\right)^{2/3}\right)$	$c_{sTT1} = 4.9$, $c_{sTT2} = 2.2$	Andreas (1988) [a]
$c_{sTT1}\left(1 + c_{sTT2}\frac{z-d}{L_{MO}}\right)$	$c_{sTT1} = 4.9$, $c_{sTT2} = 0$	de Bruin *et al.* (1993)
$4k^{-2/3}\beta_1\left(1 + c_{TT2}\frac{z-d}{L_{MO}} + c_{TT3}\left(\frac{z-d}{L_{MO}}\right)^2\right)^{1/3}$	$\beta_1 = 0.86$, $c_{TT2} = 7$, $c_{TT3} = 20$	Thiermann and Grassl (1992) [b]

[a] adjustment of Wyngaard (1973) reflecting the change of Von Karman constant from 0.35 to 0.4
[b] β_1 is the Obukhov-Corrsin constant, k is the Von Karman constant

Table 4.2: Overview of similarity relationships $\Phi_{TT}\left(\frac{z-d}{L_{MO}}\right) = C_{T^2}\theta_*^{-2}(z-d)^{2/3}$ for stable conditions.

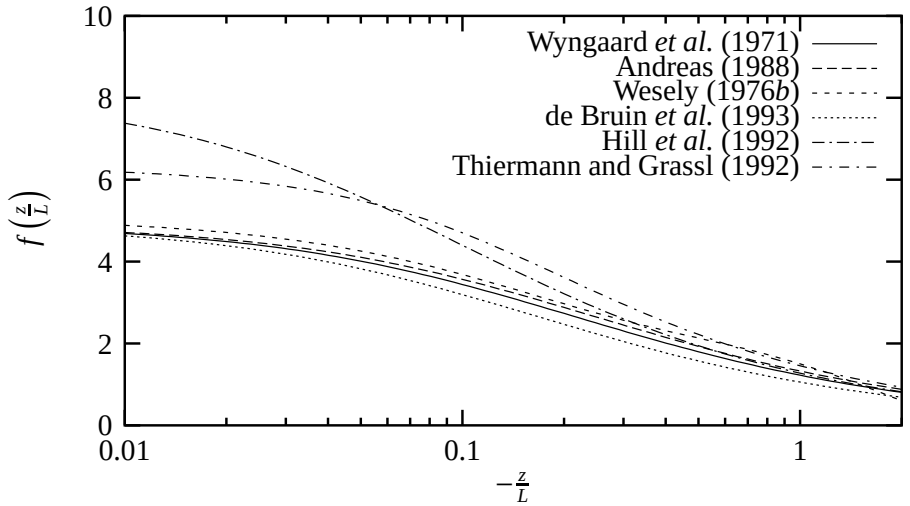

Figure 4.1: Comparison of various similarity functions $\Phi_{TT}\left(\frac{z-d}{L_{MO}}\right) = C_{T^2}\theta_*^{-2}(z-d)^{2/3}$ for unstable conditions. See table 4.1 for the expressions used.

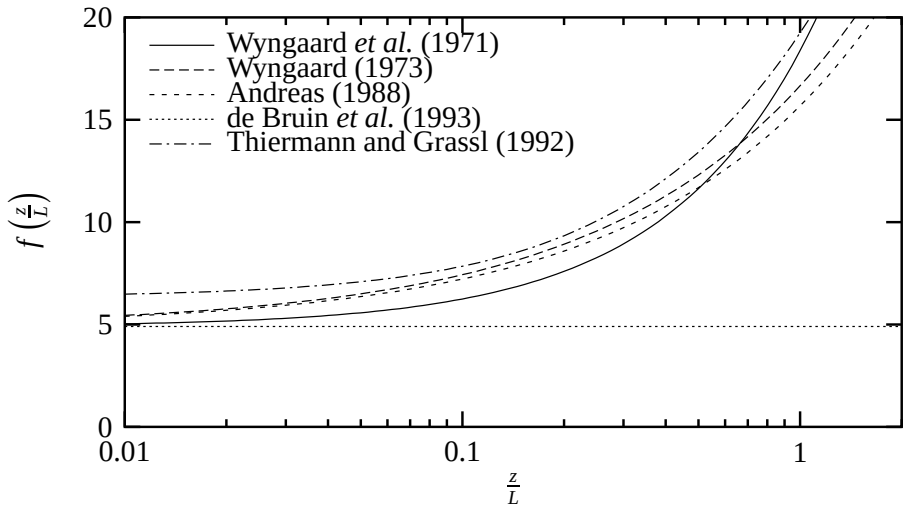

Figure 4.2: Comparison of various similarity functions $\Phi_{TT}\left(\frac{z-d}{L_{MO}}\right) = C_{T^2}\theta_*^{-2}(z-d)^{2/3}$ for stable conditions. See table 4.2 for the expressions used.

or in combination with and estimate for the roughness length):

$$u_* = \frac{k(u_2 - u_1)}{\ln\left(\frac{z_2-d}{z_1-d}\right) - \Psi_m\left(\frac{z_2-d}{L_{MO}}\right) + \Psi_m\left(\frac{z_1-d}{L_{MO}}\right)} \tag{4.4}$$

with:

$$\Psi_m\left(\frac{z-d}{L_{MO}}\right) = \int_0^{\frac{z-d}{L_{MO}}} \left(\frac{1-\phi_m(\zeta)}{\zeta}\right) d\zeta \,, \tag{4.5}$$

where $\phi_m\left(\frac{z-d}{L_{MO}}\right)$ is the flux profile relationship for momentum ($\phi_m = \frac{k(z-d)}{u_*}\frac{\partial \overline{u}}{\partial z}$). In (4.4) u_1 can be taken as zero, if z_1 is replaced by the roughness length, i.e. $z_0 + d$. The sensible heat flux can be determined iteratively from the combination of (4.1), (4.2), (4.3) and (4.4).

For unstable situations various authors have looked at the free convection limit of (4.1) (i.e. $-\frac{z-d}{L_{MO}} \rightarrow \infty$). For those expressions for $\Phi_{TT}\left(\frac{z-d}{L_{MO}}\right)$ that have the form $\Phi_{TT}\left(\frac{z-d}{L_{MO}}\right) = c_{TT1}\left(1 - c_{TT2}\frac{z-d}{L_{MO}}\right)^{-2/3}$ this leads to the following explicit expression for H (see also de Bruin *et al.* (1995)):

$$\begin{aligned} H &= \rho c_p c_{TT1}^{-3/4} c_{TT2}^{1/2} k^{1/2}(z-d)\left(\frac{g}{\overline{T}}\right)^{1/2} C_{T^2}^{3/4} \\ &= \rho c_p b(z-d)\left(\frac{g}{\overline{T}}\right)^{1/2} C_{T^2}^{3/4} \end{aligned} \tag{4.6}$$

Equation (4.6) provides a way to compute the sensible heat flux without the need for an estimate for u_* and without the need for an iterative procedure. In practice it appears that the free convection approximation is valid already at relatively modest values of $\frac{z-d)}{L_{MO}}$. de Bruin *et al.* (1995) show that the difference between the full set of equations for H and the free convection approximation is less than 10% if $-\frac{z-d}{L_{MO}} > 0.5$. It is important to note that a large z/L_{MO} can not only be obtained through a small L, but also through a large z, i.e. when the LAS is installed at a considerable height. From (4.6) it can be seen that for a given heat flux, C_{T^2} (and consequently C_{n^2}) decreases with height. This suggests that saturation (see (2.6.2) in section 2.6.2) can be prevented by installing the LAS at a sufficient height (which gas the additional advantage that free convection conditions are more easily obtained.

de Bruin *et al.* (1993) provide an explicit approximation to compute the sensible heat flux for the entire unstable range. From (4.1) a general proportionality can be inferred between H on one hand, and $\sqrt{C_{T^2}}$ and some velocity scale on the other hand:

$$H \sim \sqrt{C_{T^2}} u'_* \,, \tag{4.7}$$

where u'_* is an undefined velocity scale. de Bruin *et al.* approximate u'_* with an interpolation between the neutral friction velocity (that can be derived from the logarithmic wind profile) and a free convection velocity scale. This leads to:

$$H = \rho c_p \frac{\sqrt{C_{T^2}(z-d)^{2/3}}}{c_{TT1}} \left(u_{*n}^{1/p} + u_c^{1/p}\right)^p \,, \tag{4.8}$$

with:

$$u_{*n} = \frac{k\overline{u}(z_u)}{\ln((z_u - d)/z_0)} \tag{4.9}$$

$$u_c = \left(\sqrt{C_{T^2}(z-d)^{2/3}} \frac{kg(z-d)}{\overline{T}} \frac{c_{TT2}}{c_{TT1}}\right)^{1/2} \,, \tag{4.10}$$

where z_u and z_T are the heights where $\overline{u}$ and C_{T^2} are measured, respectively. The value of the exponent p does depend on z_u, z_T and z_0, but typical values are between 2 and 2.5.

4.3 Data required to compute the sensible heat flux

In this section the data requirements for the calculation of the sensible heat flux from LAS data will be dealt with.

Table 4.3 summarizes all variables and parameters needed to derive the sensible heat flux from the primary output of a scintillometer, i.e. the log-intensity variance. A number of the variables listed are not very crucial in the determination of the sensible heat flux, in the sense that H is not very sensitive to them. This holds in particular for $\overline{T}$, $\overline{q}$, $\overline{p}$. For a given situation these variables can usually safely be treated as parameters. The information about the relationship between humidity fluctuations and temperature fluctuations (R_{Tq} in combination with either β or $\frac{\sigma_T}{\sigma_q}$) could be replaced by a fixed value if it is assumed that the state of the surface in terms of energy partitioning between H and $L_v E$ does not change significantly. However, it is important to note that for Bowen ratios less than 0.5 to 1 the correction term should not be neglected. The influence either u_* or $\overline{u}$ diminishes as soon as a state of free convection is reached.

The parameters listed in 4.3 can be divided into three categories:

a. Parameters that are directly related to the LAS, i.e. D and λ. These will be known quite accurately.

b. Parameters that are related to the installation of LAS, i.e. z_T and L (and d). In practice, these two parameters cause significant problems in their determination, whereas they are at the same time of prime importance in the accurate calculation of H (see (2.34) and (4.6) according to which $H \sim L^{-9/4}$ and $H \sim (z-d)$. Especially over undulating terrain the determination of the correct z_T is non-trivial.

c. Parameters that are related to the estimation of u_*, i.e. z_u, z_0 (and d). For situations approaching the free convection limit the influence of these parameters vanishes. Note that situations of free convection are easily obtained in the case that z_T is large.

type	quantity	symbol	needed for
variable	log intensity variance	$\sigma^2_{ln(I)}$	C_{n^2}
	mean absolute temperature	$\overline{T}$	A_T, A_q, in similarity relationships (in $\frac{g}{\overline{T}}$)
	mean specific humidity	$\overline{q}$	A_q
	mean atmospheric pressure	$\overline{p}$	A_T, A_q
	friction velocity	u_*	$\frac{z-d}{L_{MO}}$ and θ_*
	mean wind speed	$\overline{u}$	for u_* (if no direct measurement of u_* available)
	ratio of standard deviations of temperature and humidity	$\frac{\sigma_T}{\sigma_q}$	link between C_{n^2} and C_{T^2}
	Bowen ratio	β	link between C_{n^2} and C_{T^2} (if $\frac{\sigma_T}{\sigma_q}$ not available)
	correlation coefficient between temperature and humidity	R_{Tq}	link between C_{n^2} and C_{T^2}
parameter	displacement height	d	in similarity relationships
	roughness length	z_0	for u_* (if no direct measurement of u_* available)
	height of wind speed measurement	z_u	for u_* (if no direct measurement of u_* available)
	path height	z	in similarity relationships
	path length	L	for C_{n^2}
	beam diameter	D	for C_{n^2}
	wavelength of light	λ	for C_{n^2}

Table 4.3: Variables and parameters that are needed *in principle* to derive the sensible heat flux from LAS data. The sensitivity of H to a large number these variables is small, and the variables can be treated as parameters with a fixed estimated value.

5 Conclusion and discussion

In the present paper it has been discussed in which way the output of a Large Aperture Scintillometer (LAS) can be used to determine the sensible heat flux. The link between the output of the scintillometer, i.e. the variance of the log-amplitude of the optical signal, and the sensible heat flux consists of a number of steps:

a. The structure function parameter of the refractive index C_{n^2} can be linked to the log-amplitude variance through a number of assumptions with respect to the spectrum of the turbulence along the scintillometer path. Also some requirements with respect to the relationship between wave length, path length and beam diameter do exist.

b. The next step is to relate the structure function parameter of the refractive index to the structure function parameter of temperature. To this end one needs on one hand information about the mean state of the atmosphere along the path of the scintillometer. On the other hand knowledge is required about the relative magnitude of temperature and humidity fluctuations, as well as on their mutual correlation. The latter information will in general not be available.

c. Finally, the Monin-Obukhov similarity relationship for C_{T^2} is used to express the sensible heat flux –in most cases implicitly– in terms of C_{T^2}.

The steps **b** and **c** contain the weakest links in the estimation of H from scintillometer data.

The correction for the influence of water vapour fluctuations on the relationship between C_{n^2} and C_{T^2} consists of information about the ratio between the magnitude of temperature and humidity fluctuations, σ_T/σ_q, and the correlation coefficient between temperature and humidity fluctuations, R_{Tq}. Under stationary and horizontally homogeneous conditions [1] the picture is relatively simple. Either σ_T/σ_q (or equivalently the Bowen ratio) is large in which case the the correction for the influence of water vapour fluctuations on the relationship between C_{n^2} and C_{T^2} is small (see figure 3.2). Under these conditions the value of $|R_{Tq}|$ is irrelevant and might be below one (e.g. due to entrainment effects, see de Bruin *et al.* (1999)). On the other hand, the Bowen ratio might be low and the correction may be significant (up to 50 %). But in those cases the correlation coefficient R_{Tq} will be close to one in general. In the situation that non-stationarity or inhomogeneity plays a role, since in that case R_{Tq} can take any value (see de Bruin *et al.* (1999)). It is important to note that in the derivation of the water vapour correction no use is made of assumptions concerning similarity relationships. With respect to the water vapour fluctuations one issue has not been touched upon, viz. the influence of absorption of radiation by water vapour which may also give rise to fluctuations in the intensity measured at the receiver (see e.g. Nieveen *et al.* (1998)).

The second weak link in the determination of the sensible heat flux from scintillometer data are the similarity relationships used. First there is considerable scatter in the similarity relationships themselves. For unstable conditions these differences may give a difference in flux (assuming free convection conditions) of nearly 20% between the highest and the lowest. Furthermore, the similarity relationships may not be valid under all conditions. In principle they have been derived for conditions that are stationary and horizontally homogeneous. There is some evidence that also over inhomogeneous terrain the the sensible heat flux given by the LAS is representative for the areally averaged flux (Wouter Meijninger, personal communication).

[1] For these conditions, Monin-Obukhov Similarity (MOS) is supposed to be valid. But Hill (1989) shows that MOS implies that $|R_{Tq}| = 1$.

The main conclusion of this paper is that the scintillation method is a powerful method to measure the sensible heat flux, but there are a large number of pitfalls that can easily be circumvented if given sufficient attention. On the other hand there are some difficulties that should receive more attention and that can not be circumvented always (viz. the influence of water vapour fluctuations and the validity of similarity relationships).

Bibliography

Andreas E.L. (1988). Estimating C_n^2 over snow and seas ice from meteorological data. *J. Opt. Soc. Am.*, 5, 481–495.

Bendat J. and Piersol A. (1986). *Random data: analysis and measurement procedures*. John Wiley & Sons, 2^{nd} edn.

de Bruin H.A.R., van den Hurk B.J.J.M. and Kohsiek W. (1995). The scintillation method tested over a dry vineyard area. *Boundary-Layer Meteorol.*, 76, 25–40.

de Bruin H.A.R., van den Hurk B.J.J.M. and Kroon L.J.M. (1999). On the temperature-humidity correlation and similarity. *Boundary-Layer Meteorol.*, 93, 453–468.

de Bruin H.A.R., Kohsiek W. and van den Hurk B.J.J.M. (1993). A verification of some methods to determine the fluxes of momentum, sensible heat, and water vapour using standard deviation and structure parameter of scalar meteorological quantities. *Boundary-Layer Meteorol.*, 63, 231–257.

Clifford S., Ochs G. and Lawrence R. (1974). Saturation of optical scintillation by strong turbulence. *J. Opt. Soc. Am.*, 64, 148–154.

Corrsin S. (1951). On the spectrum of isotropic temperature fluctuations in an isotropic turbulence. *J. Appl. Phys.*, 22, 469–473.

Feynman R.P., Leighton R.B. and Sands M.L. (1989). *The Feynman Lectures on Physics: Commemorative Issue*. Addison-Wesley Publishing Company Inc., Reading, Massachusetts.

Friehe C.A., La Rue J.C., Champagne F.H., Gibson C.H. and Dreyer G.F. (1975). Effects of temperature and humidity fluctuations on the optical refractive index in the marine boundary layer. *J. Opt. Soc. Am.*, 65, 1502–1511.

Goody R.M. (1965). *Atmospheric Radiation*, vol. 1. Clarendon, Oxford.

Hartogensis O., de Bruin H. and van de Wiel B. (2002). Displaced-beam small aperture scintillometer test. part II: CASES-99 stable boundary-layer experiment. *Boundary-Layer Meteorol.*, 105, 149–156.

Hill R. (1978*a*). Models of the scalar spectrum for turbulent advection. *J. Fluid Mech.*, 88, 541–562.

Hill R. and Ochs G. (1978). Fine calibration of large-aperture optical scintillometers and an optical estimate of inner scale of turbulence. *Applied Optics*, 17, 3608–3612.

Hill R.J. (1978*b*). Spectra of fluctuations in refractivity, humidity, and the temperature-humidity cospectrum in the inertial and dissipation range. *Radio Science*, 13, 953–961.

Hill R.J. (1989). Implications of Monin-Obukhov similarity theory for scalar quantities. *J. Atmos. Sci.*, 46, 2236–2251.

Hill R.J., Clifford S.F. and Lawrence R.S. (1980). Refractive-index and absorption fluctuations in the infrared caused by temperature, humidity, and pressure fluctuations. *J. Opt. Soc. Am.*, 70, 1192–1205.

Hill R.J., Ochs G.R. and Wilson J.J. (1992). Measuring surface-layer fluxes of heat and momentum using optical scintillation. *Boundary-Layer Meteorol.*, 58, 391–408.

Hoedjes J.C.B., Zuurbier R.M. and Watts C.J. (2002). Applicability of a large aperture scintillometer (LAS) over a homogeneous irrigated area partly affected by regional advection. *Boundary-Layer Meteorol.*, 105, 99–117.

van de Hulst H. (1981). *Light scattering by small particles*. Dover Publications, Inc., New York.

Jenkins F. and White H. (1976). *Fundamentals of optics*. McGraw-Hill, New York, etc., 4th edn.

Kohsiek W. (1982). Measuring C_T^2, C_Q^2, and C_{TQ} in the unstable surface layer, and relations to the vertical fluxes of heat and moisture. *Boundary-Layer Meteorol.*, 24, 89–107.

Kohsiek W. (1984). Inertial subrange correlation between temperature and humidty fluctuations in the unstable surface layer above vegetated terrains. *Boundary-Layer Meteorol.*, 29, 211–224.

Kohsiek W. and Herben M.H.A.J. (1983). Evaporation derived from optical and radio-wave scintillation.

Appl. Opt., 22, 2566–2570.

Kohsiek W., Meijninger W., Moene A., Heusinkveld B., Hartogensis O., Hillen W. and de Bruin H. (2002). An extra large aperture scintillometer (XLAS) with a 9.8km path length. *Boundary-Layer Meteorol.*, 105, 119 – 127.

Kolmogorov A. (1941*a*). Dissipation of energy in the locally isotropic turbulence. *C.R. Acad. Sci. URSS*, 32, 16.

Kolmogorov A. (1941*b*). The local structure of turbulence in incompressible viscous fluid for very large reynolds numbers. *C. R. Acad. Sci. URSS*, 30, 301–305.

Lee R. and Harp J. (1969). Weak scattering in random media, with applications to remote probing. *Proceedings of the IEEE*, 57, 375–406.

List R.J. (1971). *Smithsonian Meteorological Tables*. Smithsonian Institution Press, City of Washington.

McCartney E.J. (1976). *Optics of the Atmosphere - Scattering by Molecules and Particles*. John Wiley & Sons, New York etc.

Meijninger W.M.L., Green A., Hartogensis O., Hoedjes J., Zuurbier R. and de Bruin H. (2002*a*). Determination of area averaged water vapour fluxes with a large aperture and radio wave scinillometer over a heterogeneous surface - flevoland experiment. *Boundary-Layer Meteorol.*, 105, 63–83.

Meijninger W.M.L., Hartogensis O.K., Kohsiek W., Hoedjes J.C.B., Zuurbier R.M. and de Bruin H.A.R. (2002*b*). Determination of area-averaged sensible heat fluxes with a large aperture scintillometer over a heterogeneous surface - flevoland field experiment. *Boundary-Layer Meteorol.*, 105, 37–62.

Moene A.F. (2003). Effects of water vapour on the structure parameter of the refractive index for near-infrared radiation. *Boundary-Layer Meteorol.*, 107, 635 – 653.

Monin A. and Yaglom A. (1971). *Statistical fluid mechanics: mechanics of turbulence*, vol. Volume 1. The MIT Press, Cambridge etc.

Nieveen J.P., Green A.E. and Kohsiek W. (1998). Using a large-aperture scintillometer to measure absorption and refractive index fluctuations. *Boundary-Layer Meteorol.*, 87, 101–116.

Obukhov A.M. (1949). Structure of the temperature field in a turbulent current. *Izv. Akad. Nauk SSSR, Series Geograf i Geofiz*, 13, 58–69.

Ochs G., Clifford S. and Wang T. (1976). Laser wind sensing: the effects of saturation of scintillation. *Applied Optics*, 15, 403–408.

Ochs G. and Wang T. (1978). Finite aperture optical scintillometer for profiling wind and C_{n^2}. *Applied Optics*, 17, 3774–3778.

Owens J.C. (1967). Optical refractive index of air: Dependence on pressure, temperature and composition. *Appl. Opt.*, 6, 51–59.

Strohbehn J. (1968). Line-of-sight wave propagation through the turbulent atmosphere. *Proceedings of the IEEE*, 56, 1301–1318.

Tatarski V. (1967). *Propagation of waves in a turbulent atmosphere*. Nauka, Moscow. (in Russian).

Tatarskii V. (1961). *Wave propagation in a turbulent medium*. McGraw-Hill Book Company Inc., New York.

Thiermann V. and Grassl H. (1992). The measurement of turbulent surface-layer fluxes by use of bichromatic scintillation. *Boundary-Layer Meteorol.*, 58, 367–389.

Wang T., Ochs G. and Clifford S. (1978). A saturation-resistant optical scintillometer to measure C_n^2. *J. Opt. Soc. Am.*, 68, 334–338.

Wesely M.L. (1976*a*). The combined effect of temperature and humidity fluctuations on refractive index. *J. Appl. Meteor.*, 15, 43–49.

Wesely M.L. (1976*b*). A comparison of two optical methods for measuring line averages of thermal exchanges above warm water surfaces. *J. Appl. Meteor.*, 15, 1177–1188.

Wesely M.L. and Alcaraz E.C. (1973). Diurnal cycle of the refractive index structure function coefficient. *J. Geophys. Res.*, 78, 6224–6232.

Wyngaard J.C. (1973). On surface-layer turbulence. In: Haugen D.A. (ed.), *Workshop on Mircometeorology*, pp. 101–149, Boston, Mass. American Meteorological Society.

Wyngaard J.C., Izumi Y. and Collins S.A. (1971). Behavior of the refractive-index structure parameter near the ground. *J. Opt. Soc. Am.*, 61, 1646–1650.

Wyngaard J.C., Pennell W.T., Lenshow D.H. and LeMone M.A. (1978). The temperature-humidity covariance budget in the convective boundary-layer. *J. Atmos. Sci.*, 35, 47–58.